# A flavour of family symmetries in a family of flavour models

Adelhart Toorop, R. de

# Chapter 5

# Flavour symmetries at the electroweak scale

For there are three that bear record in heaven,
[...]: and these three are one.

*The Bible - King James Version*
*1 John 5:7*

## 5.1 Introduction

When studying the Altarelli–Feruglio model in chapter 2 we found that the mass scale of flavons of flavour symmetries is typically very high. It can be as high as the assumed energy scale of grand unification. In the previous chapter, we used this to our advantage and constructed a model that contains both grand unified and family symmetries. The disadvantage is that the model is not very predictive. There is a limited effect of the physics at the very high scale on the physics at scales that the current experiments are investigating, the TeV scale for the LHC and even lower scales for neutrino experiments. There are some predictions, for instance about the rates of neutrinoless double beta decay and the presence at the SUSY scale of extra doubly charged scalars $\delta^{++}$ and $\bar{\delta}^{--}$, but these are not very many. The predictiveness of flavour models is significantly enlarged if the scale of symmetry breaking can be lowered to the electroweak scale. In this chapter we study a set up in which this is indeed the case.

The flavour model of the previous section contained flavons and pure Higgs fields. Flavons are scalar fields that are singlets of the SM gauge group, but charged under the family symmetry group, while for pure Higgs fields it is exactly the other way around. The central idea of this chapter, introduced in section 5.2, is to combine these two fields to form 'flavo-Higgses' that are in non-trivial representations of both the flavour symmetry group and the electroweak group. Naturally, breaking electroweak symmetry also implies breaking the flavour symmetry and we obtain low-energy, highly predictive models of flavour.

In particular we are interested in models where there are three Standard-Model like Higgs fields that are in the triplet representation of the family symmetry group $A_4$. In section 5.3 we introduce this scenario and in section 5.4 we present the corresponding potential for the flavo-Higgs fields. Section 5.5 discusses the physical Higgs fields present after breaking electroweak symmetry.

The potential of section 5.4 allows only a limited number of minima. In section 5.6 we construct a complete list of all those vacua and in section 5.7 we discuss the question whether in these cases CP is violated in the Higgs sector. The vacua are solutions of the mathematical equations that minimize the potential. The question whether they are also physically viable is a different one. In section 5.8 we develop a number of tests that are only sensitive to the Higgs sector of a model and in section 5.9

we confront the minima of section 5.6 with these tests.

To constitute a complete model, knowledge of the representation of the Higgs fields (an $A_4$-triplet), is not enough. Only when also the fermionic content is given a complete model arises. In section 5.10 we present four such models, three from the literature and one original work, called 'quark mixing in the discrete dark matter model'. In section 5.11 we present a number of tests for these models that are sensitive also to the fermionic content and in section 5.12 we present the results of these tests. Lastly, section 5.13 presents the conclusions.

## 5.2 The pros and cons of flavons

The crucial assumption of models with flavour symmetries is the existence of a horizontal gauge group. Invariance under this flavour group dictates which terms are allowed in the Lagrangian of the resulting field theory. The Lagrangian of the Standard Model, equation (2.1), is well-known

$$\mathcal{L}_{\text{SM}} = \mathcal{L}_K + \mathcal{L}_{\text{gauge}} + \mathcal{L}_Y + V_{\text{Higgs}}.$$

Typically, adding a family symmetry group does not affect the kinetic and gauge terms, as the usual choice is not to gauge the flavour group. The effect on the Yukawa terms, on the other hand, is drastic. The terms originally present in the Standard Model are not invariant under the flavour group. In chapters 2 and 4 we have seen ways to fix this deficit and we found that the way in which invariance is recovered ultimately dictates what the masses and mixing angles of the fermions look like. A crucial choice is whether the last term $V_{\text{Higgs}}$ is to be modified as well.

In the previous chapters, the solution to make the Yukawa terms invariant, was to introduce flavons. These fields transform trivially under (vertical) gauge transformations, but are in extended representations of the flavour symmetry. The flavons acquire vacuum expectation values and the structure of the vevs translates to structures in the fermion mass matrices. The Higgs sector on the other hand, was touched as little as possible. In the Altarelli–Feruglio model the Higgs fields are singlets of the family symmetry and in the Pati-Salam inspired model of chapter 4, they transform under the auxiliary $Z_4$, but are still singlets of the $S_4$ symmetry.

Modifications of the Higgs potential in the strict sense are absent in the model of Altarelli and Feruglio. The point that they are larger than naively expected in the model of chapter 4 is one of the main messages of that chapter. Still, the modifications are relatively limited when compared to a scenario where the Higgses are not only charged under $Z_4$, but also under $S_4$.

The addition 'in the strict sense' in the previous paragraph refers to the fact that the non-modification concerns the potential of the 'traditional' Higgses, i.e. the fields that break electroweak (ew) symmetry. The flavons are also fields that break a symmetry – in this case the family symmetry. To write down a mass term for fermions, both electroweak Higgses and flavons are needed. It can thus be well defended to see the flavons as a second type of Higgs fields. From this point of view, there is a very significant modification of the Higgs potential

$$V_{\text{Higgs}} \longrightarrow V_{\text{ew Higgs}} + V_{\text{Flavons}} \,. \tag{5.1}$$

In the previous chapters, we have seen that the idea of using flavons is quite attractive. It is possible to build models that reproduce the tribimaximal or bimaximal mixing patterns, without having to tune parameters. However, four weaker points of the approach should also be stressed.

Firstly, non-renormalizable operators are ubiquitous in models with flavons. Several flavons are added to Yukawa couplings that originally exactly had dimension 4. We discussed the effective Weinberg-operator for neutrino masses and its possible origin from one of the three types of seesaw (or a combination thereof) in chapter 2 and concluded that non-renormalizable interactions are in principle no problem for a theory. Still, their appearance makes the theory significantly more complicated.

Secondly, models can be quite baroque. In the set up of chapter 4, no fewer than nine new flavon fields had to be introduced. The flavons $\varphi$ and $\varphi'$ are tailored to couple to charged fermions at leading order, while $\chi$ and $\sigma$ couple to neutrinos. The four driving fields do not even couple to the SM fermions directly, but are needed to help the other flavons obtain the correct vevs. The Froggatt–Nielsen messenger lastly ensured the fermion hierarchy. All flavons fulfill a well-defined role and none of them is redundant. The number nine thus seems to be rather minimal for this type of models, but it is quite large. It is worth trying to see if simpler models with flavour symmetry can be constructed.

Thirdly, all the known techniques for flavon alignment in case of more than one flavon require supersymmetry or the presence of extra dimensions. These are two types of new physics that are very well-motivated. They explain one of the greatest standing puzzles in the Standard Model, the hierarchy problem of section 1.3.2 and, as a bonus, give a dark matter candidate. Supersymmetry at the TeV scale furthermore enables gauge unification as shown in section 1.3.3. There are thus good arguments to include supersymmetry or extra dimensions in flavour model building, but it would be preferable not to depend on them and to be able to write down more minimal models. This is especially true in a time where the experimental bounds on supersymmetry (or at least on the simplest implementations of it) are becoming rather tight.

Lastly, the scale of the physics of the flavons is typically very high. In the Altarelli–Feruglio model, the cut-off scale is estimated to be of the order of $10^{15}$ GeV; in the model of section 4 it should be the GUT scale. This can be read from figure 4.7 and 4.8 to be of the order of $10^{13}$ GeV. An advantage of this high scale is that it is possible to build models that combine flavour and grand unified symmetries. The downside is that the theories are hard to test and that few direct predictions can be made. An effect on neutrino parameters is present as shown in section 4.11, but direct detection of the flavons is out of the question.

In this chapter, we discuss an alternative possibility. We assume that there are no separate flavons, but that the Standard Model Higgs field takes their role. In this 'flavo-Higgs' set up, there are three copies of the SM Higgs that are in a triplet of the flavour group. Once the Higgses get their vevs, the resulting 'vector of vevs' acts as the flavons.

In this set up, the four weak points described above are ameliorated. All couplings are of the Yukawa type fermion-fermion-Higgs and are thus renormalizable. Although there is a substantial amount of new fields (two extra copies of the Higgs field), this is far less than in the other models. The alignment in flavour space is now possible in a non-supersymmetric context and without extra dimensions; all that is required is finding the vacuum expectation values of the three Higgses. The scale of new physics is obviously the electroweak scale and the set up is thus testable at the LHC by direct detection of the extra Higgs fields and verification that they have the right couplings. The indirect tests also become numerous. These can in fact be used to constrain the models significantly.

The disadvantage is that we only have one (effective) flavon. This limits the amount of structure we can impose on the fermion masses. For instance, to reproduce the exact tribimaximal mixing pattern, we need to tune one parameter. This is still much better than in the Standard Model, where the tuning of three parameters (all three neutrino mixing angles) is required.

## 5.3 The three Higgs doublet scenario

In this chapter we investigate a flavo-Higgs set up. The most important choice to make is that of the family symmetry group. We choose the group $A_4$. This group is very well-known in particular in models with flavons. The Altarelli–Feruglio model of section 2.4 used $A_4$ to reproduce tribimaximal mixing in the lepton sector, although in section 3.3.1 it was shown that this requires the appearance of an additional accidental $Z_2$ symmetry.

The fact that an accidental symmetry was required to give a specific mixing pattern is valuable information when constructing a flavo-Higgs model. In the previous section it was shown that this

set up can produce only one direction in flavour space. Residual symmetries in the neutrino and charged lepton sector (the key for finding mixing patterns in chapter 3) will necessarily be severely limited. If accidental symmetries can realize a mixing pattern even when certain directions in flavour space are not given by flavon vevs, that is good news.

Throughout this chapter, we work in the $S$-diagonal basis, often referred to as the Ma-Rajasekaran basis. The transformations from this basis to the $T$-diagonal basis of Altarelli and Feruglio as well as all other details of the group theory of $A_4$ is given in appendix 3.A. We recall that the group has a trivial as well as two non-trivial one-dimensional representations (1, $1'$ and $1''$) and one three-dimensional representation (3). In order to provide a non-trivial direction in flavour space, the flavo-Higgs fields should thus transform as a triplet of $A_4$. We adopt the standard notation to refer to these fields as $\Phi$ instead of $H$.

$$\vec{\Phi} = (\Phi_1,\, \Phi_2,\, \Phi_3) \tag{5.2}$$

We stress that each of the Higgs fields has the same hypercharge $+1/2$ as the fields $H_d$ of chapter 2. Our set up is thus very different from the MSSM, that has multiple (two) Higgs doublets, but these have different hypercharges. In the language of chapter 2, the Higgs sector in this chapter is characterized by $n_u = 0$ and $n_d = 3$.

Each of these Higgs fields is written in terms of $SU(2)_L$ components and expanded around its vacuum expectation value similar to equation (2.4)

$$\Phi_a \to \frac{1}{\sqrt{2}} \begin{pmatrix} \text{Re}\, \phi_a^1 + i\, \text{Im}\, \phi_a^1 \\ v_a e^{i\omega_a} + \text{Re}\, \phi_a^0 + i\, \text{Im}\, \phi_a^0 \end{pmatrix}. \tag{5.3}$$

Here $v_a e^{i\omega_a}$ is the vacuum expectation value of the $a^{\text{th}}$ Higgs field. One or two of the $v_a$ can be zero, implying that the corresponding Higgs field does not develop a vev. The phases $\omega_a$ appears due to the fact that the vacuum expectation values can generally be complex. A global rotation can remove one phase, so in a one-Higgs doublet model the vev is generally chosen real. In models with more than one Higgs doublet, phases carry physical information and should be taken into account. Note that the appearance of complex vevs does not automatically imply CP violation. For a discussion of CP violation in the Higgs sector, see section 5.7.

Next to these three Higgs fields, there may be additional Higgses in one of the one-dimensional representations. We refer to models with only the $A_4$ triplet Higgs as minimal and to models that also have singlets as non-minimal. In this section we investigate the potential and its vacua solutions for the minimal set up. Two of the models we discuss in section 5.10 are indeed minimal, while two others are non-minimal.

In this chapter the $A_4$ representation for the Higgs fields is now fixed. The choice of representation for the various fermions is still free. The requirement that the SM Yukawa couplings can still be written down requires at least one of the fermion fields to be in the triplet representation. Whether this is the left- or the righthanded field and if fields in one-dimensional representations are in 1, $1'$ or $1''$ is a further choice to be made. In this chapter we perform several tests of the viability of a certain situation. Tests that only take the Higgs sector into consideration and that are thus insensitive to choices made in the fermion representations are referred to as 'model-independent' tests, while tests that involve fermions are 'model-dependent' tests.

## 5.4 The $A_4$ invariant Higgs potential

The Higgs potential of the ordinary Standard Model Higgs as given below equation (2.19) is the well-known 'Mexican hat' potential.

$$V(H) = \mu^2 H^\dagger H + \lambda (H^\dagger H)^2$$

The coefficients $\mu^2$ and $\lambda$ of the quadratic and quartic terms are respectively negative and positive. This keeps the potential bounded from below, while having a non-trivial minimum to break electroweak symmetry.

The Higgs potential in the three Higgs doublet model with $A_4$ symmetry is constructed in the same spirit. It contains quadratic and quartic terms in the Higgs fields. The group theory of $SU(2)$ and $A_4$ dictates that only one quadratic term is possible, while there are several ways to contract the indices in the quartic terms. As shown by Ma and Rajasekaran [97], the most general potential is given by

$$\begin{aligned} V[\Phi_a] =& \mu^2(\Phi_1^\dagger\Phi_1 + \Phi_2^\dagger\Phi_2 + \Phi_3^\dagger\Phi_3) + \lambda_1(\Phi_1^\dagger\Phi_1 + \Phi_2^\dagger\Phi_2 + \Phi_3^\dagger\Phi_3)^2 + \\ &+ \lambda_3(\Phi_1^\dagger\Phi_1\Phi_2^\dagger\Phi_2 + \Phi_1^\dagger\Phi_1\Phi_3^\dagger\Phi_3 + \Phi_2^\dagger\Phi_2\Phi_3^\dagger\Phi_3) + \\ &+ \lambda_4(\Phi_1^\dagger\Phi_2\Phi_2^\dagger\Phi_1 + \Phi_1^\dagger\Phi_3\Phi_3^\dagger\Phi_1 + \Phi_2^\dagger\Phi_3\Phi_3^\dagger\Phi_2) + \\ &+ \frac{\lambda_5}{2}\left[e^{i\epsilon}\left[(\Phi_2^\dagger\Phi_1)^2 + (\Phi_3^\dagger\Phi_2)^2 + (\Phi_1^\dagger\Phi_3)^2\right] + e^{-i\epsilon}\left[(\Phi_1^\dagger\Phi_2)^2 + (\Phi_2^\dagger\Phi_3)^2 + (\Phi_3^\dagger\Phi_1)^2\right]\right]. \end{aligned} \tag{5.4}$$

The parameters $\lambda_{1,3,4,5}$ and $\epsilon$ are chosen to be in accordance with the usual notation in two Higgs doublet models [125, 126]. The parameter $\mu^2$ is typically negative in order to have a stable minimum away from the origin. All the other parameters, $\lambda_i$, are real parameters which are subject to the condition that the potential is bounded from below: this forces $\lambda_1$ and the combination $\lambda_1 + \lambda_3 + \lambda_4 + \lambda_5\cos\epsilon$ to be positive.

### 5.4.1 Soft $A_4$ breaking

When the Higgs fields develop vacuum expectation values, they break electroweak symmetry as well as the $A_4$ flavour symmetry. At that moment, $A_4$ is thus spontaneously broken. It is also possible to break $A_4$ explicitly, by adding terms to the potential that are not invariant. This is obviously against the spirit of introducing the symmetry in the first place and should thus only be done as a last resort. One way to break $A_4$ is by adding soft breaking terms to the potential (5.4) in the form

$$V_{A_4\text{soft}} = v_{\text{ew}}^2\frac{m}{2}(\Phi_1^\dagger\Phi_2 + \Phi_2^\dagger\Phi_1) + v_{\text{ew}}^2\frac{n}{2}(\Phi_2^\dagger\Phi_3 + \Phi_3^\dagger\Phi_2) + v_{\text{ew}}^2\frac{k}{2}(\Phi_1^\dagger\Phi_3 + \Phi_3^\dagger\Phi_1)\,. \tag{5.5}$$

Here $m, n, k$ are dimensionless parameters that should presumably be smaller than one. Note that the chosen $V_{A_4\text{soft}}$ is not the most general one but it prevents an accidental extra $U(1)$ factor to appear.

The soft breaking terms are needed when we study two models [127, 128] in section 5.12. These models make use of a minimum of the potential (5.4) that gives rise to unnaturally light Higgses. The addition of the terms in (5.5) solves this problem and only after this it is meaningful to test the models on their merits.

## 5.5 Physical Higgs fields

After the symmetry breaking of the Higgs fields of equation (5.3) the components of the Higgs fields become the known Goldstone bosons of the Standard Model or the charged and neutral Higgs bosons. The number of expected Higgs bosons can easily be calculated. In the charged sector, we have three complex or six real degrees of freedom. Two of these relate to the Goldstone bosons that are eaten by the $W^+$ and $W^-$ bosons, leaving four degrees of freedom to produce two pairs of a positively and a negatively charged boson. In the neutral sector only one of the six degrees of freedom corresponds to an eaten Goldstone boson (by the $Z$ boson), leaving five neutral Higgses. In the case where all vevs are real, it is easy to see that three of these have a scalar and two a pseudoscalar nature. In this counting the assumption was made that only electroweak symmetry gets broken; there are no additional (global) broken symmetries. If those are present, extra Goldstone bosons appear and some of the Higgs states are massless.

The mixing of the six neutral states to five (pseudo)scalar states and a Goldstone boson can be

parameterized as in section 2.2.5[1]

$$\begin{aligned} h_\alpha &= U_{\alpha a}\text{Re}\,\phi_a^0 + U_{\alpha(a+3)}\text{Im}\,\phi_a^0\,, \\ \pi^0 &= U_{6a}\text{Re}\,\phi_a^0 + U_{6(a+3)}\text{Im}\,\phi_a^0\,. \end{aligned} \tag{5.6}$$

Here $a = 1, 2, 3$ and $\alpha = 1 - 5$, while $\alpha = 6$ refers to the Goldstone boson that we represent as $\pi^0$.

In the situation where all vevs are real the 6 by 6 scalar mass matrix reduces to a block diagonal matrix with two 3 by 3 mass matrices leading to three CP even states and 2 CP odd states and the GB $\pi^0$.

The three charged scalars mix into two new charged massive states $h_\alpha^+$ and a charged Goldstone boson that we refer to as $\pi^+$ and that is eaten by the gauge bosons $W^+$.

$$\begin{pmatrix} h_1^+ \\ h_2^+ \\ \pi^+ \end{pmatrix} = S \begin{pmatrix} \phi_1^1 \\ \phi_2^1 \\ \phi_3^1 \end{pmatrix}\,. \tag{5.7}$$

In general, the $S$ is a complex unitary matrix. In the special case where all vevs are real, its entries are real (and it is thus an orthogonal matrix).

It is interesting to notice that, contrary to other multi Higgs (MH) scenarios, here we cannot recover the SM limit, with one light scalar and all the others decoupled and very heavy. The flavour symmetry constrains the potential parameters in such a way that the scalar masses are never independent from each other. This can be easily understood by a parameter counting: the scalar potential (5.4) presents $6$ independent parameters and the number of the physical quantities is $8$, i.e. the electroweak (EW) vev and the seven masses for the massive scalar fields.

## 5.6 Minimum solutions of the potential

In this section we investigate the minima of the potential (5.4). We assume that electromagnetism is conserved and that thus only the neutral components of the Higgs fields develop vacuum expectation values. The fields can then be developed around their vevs as given in equation (5.3).

The tool to find minima is obviously the first derivative system

$$\frac{\partial V[\Phi]}{\partial \Phi_{\mathcal{I}}} = 0\,. \tag{5.8}$$

Here $\Phi_{\mathcal{I}}$ is one of the fields Re $\Phi_a^1$, Re $\Phi_a^0$, Im $\Phi_a^1$ or Im $\Phi_a^0$. Secondly we require non negative eigenvalues of the Hessian

$$\frac{\partial^2 V[\Phi]}{\partial \Phi_{\mathcal{I}} \partial \Phi_{\mathcal{J}}}\,. \tag{5.9}$$

This means that all the physical masses are positive except those corresponding to the Goldstone bosons (GBs) that vanish.

Some of the solutions are natural in the sense that they do not require *ad hoc* values of the potential parameters; these are only constrained by requiring the boundedness at infinity and the positivity of all the physical scalar masses. The only potential parameter constrained is the bare mass term $\mu^2$ which is related to the physical electroweak (EW) vev, $v_{\text{ew}}^2 = v_1^2 + v_2^2 + v_3^2$. Others require specific relations between the dimensionless scalar potential parameters and may have extra Goldstone bosons.

Minima of the $A_4$ scalar potential are described by a vector of vevs

$$\left(v_1 e^{i\omega_1},\quad v_2 e^{i\omega_2},\quad v_3 e^{i\omega_3}\right)\,. \tag{5.10}$$

[1] As there can be no confusion, we leave the hat over the mass eigenstates $h$.

As already mentioned below equation (5.3) one or two of the $v_i$ may be zero and it is always possible to choose at least one of the vevs real. In the remainder of this section, we categorize the potential solutions in two classes: those that can have all vevs real and those for which at least one vev is inherently complex.

### 5.6.1 Analysis of solutions with only real vacuum expectation values

When all vevs are real, the first derivative system (5.8) reads

$$\begin{aligned} v_1[2(v_1^2+v_2^2+v_3^2)\lambda_1+(v_2^2+v_3^2)(\lambda_3+\lambda_4+\lambda_5\cos\epsilon)+2\mu^2] &= 0\,,\\ v_2[2(v_1^2+v_2^2+v_3^2)\lambda_1+(v_1^2+v_3^2)(\lambda_3+\lambda_4+\lambda_5\cos\epsilon)+2\mu^2] &= 0\,,\\ v_3[2(v_1^2+v_2^2+v_3^2)\lambda_1+(v_1^2+v_2^2)(\lambda_3+\lambda_4+\lambda_5\cos\epsilon)+2\mu^2] &= 0\,,\\ v_1(v_2^2-v_3^2)\lambda_5\sin\epsilon &= 0\,,\\ v_2(v_1^2-v_3^2)\lambda_5\sin\epsilon &= 0\,,\\ v_3(v_2^2-v_1^2)\lambda_5\sin\epsilon &= 0\,. \end{aligned} \tag{5.11}$$

The first three derivatives refer to the real components of $\Phi_a^0$ and the second ones to the imaginary parts. In the most general case, when neither $\epsilon$ nor $\lambda_5$ is zero, the last three equations allow two different solutions

1) $v_1 = v_2 = v_3 = v = v_{\rm ew}/\sqrt{3}$;

2) $v_1 \neq 0$ and $v_2 = v_3 = 0$ (and permutations of the indices).

The second case obviously implies $v_1 = v_{\rm ew}$. Both cases represent solutions of the first three equations as well, provided that

$$\begin{cases} \mu^2 = -(3\lambda_1+\lambda_3+\lambda_4+\lambda_5\cos\epsilon)v_{\rm ew}^2/3 & \text{for the first case.}\\ \mu^2 = -\lambda_1 v_{\rm ew}^2 & \text{for the second case.} \end{cases} \tag{5.12}$$

In these cases $\lambda_5$ can be chosen positive, as a sign can be absorbed in a redefinition of $\epsilon$.

Next, we consider the case where $\sin\epsilon$ is 0. This implies $\epsilon = 0$ or $\pi$. We can absorb the minus sign corresponding to the second case in a redefinition of $\lambda_5$ that is then allowed to span over both positive and negative values.

Assuming $v_1 \neq 0$, we can solve the first equation in (5.11) with respect to $\mu^2$. Then by substituting $\mu^2$ in the other two equations we get

$$\begin{aligned} v_2(v_1^2-v_2^2)(\lambda_3+\lambda_4+\lambda_5) &= 0\,,\\ v_3(v_1^2-v_3^2)(\lambda_3+\lambda_4+\lambda_5) &= 0\,. \end{aligned} \tag{5.13}$$

Next to the two solutions present in the general case, this system has two further possible solutions

3) $v_3 = 0, v_2 = v_1 = v_{\rm ew}/\sqrt{2}$ and permutations. This requires

$$\mu^2 = -\left(4\lambda_1+\lambda_3+\lambda_4+\lambda_5\right)v_{\rm ew}^2/4\,. \tag{5.14}$$

4) $(\lambda_3+\lambda_4+\lambda_5) = 0$. This condition implies that in the real neutral direction there is an $O(3)$ accidental symmetry that is spontaneously broken by the vacuum configuration. Indeed in this case $v_1$, $v_2$ and $v_3$ are only restricted to satisfy $v_1^2+v_2^2+v_3^2 = v_{\rm ew}^2$ and the parameter $\mu^2$ is given by $\mu^2 = -\lambda_1 v_{\rm ew}^2$. We anticipate that the spectrum of neutral Higgs states contain problematic extra Goldstone bosons.

The next four subsections are devoted to a closer look of the four minima just described. This includes a study of the masses of the physical Higgs bosons to see for which minima the spectrum is realistic. This means that all resulting masses are non-negative (no tachyons) and that the only Goldstone bosons that appear are those related to electroweak symmetry breaking. We note that the condition $\lambda_5 = 0$ allows special cases of the solutions 1) to 4), but does not give rise to new solutions. The $\lambda_5 = 0$ scenario can thus be handled in the regular subsections regarding minima 1) to 4) and does not require a separate discussion.

### 5.6.2 The Alignment $(v, v, v)$ when $\epsilon \neq 0$

In the basis chosen, the vacuum alignment $(v, v, v)$ preserves the $Z_3$ subgroup[2] of $A_4$. It is convenient to perform a basis transformation into the $Z_3$ eigenstate basis, $1, 1' \sim \omega, 1'' \sim \omega^2$, where $\omega$ was defined in section 2.4 as a cubic root of unity. The $Z_3$ eigenstates read

$$\begin{aligned} \varphi &= (\Phi_1 + \Phi_2 + \Phi_3)/\sqrt{3} \sim 1 \\ \varphi' &= (\Phi_1 + \omega\Phi_2 + \omega^2\Phi_3)/\sqrt{3} \sim \omega \\ \varphi'' &= (\Phi_1 + \omega^2\Phi_2 + \omega\Phi_3)/\sqrt{3} \sim \omega^2 \,. \end{aligned} \tag{5.15}$$

In the $Z_3$ basis, $\varphi \sim 1$ behaves like the standard Higgs doublet: its neutral real component develops a vacuum expectation values $\langle \varphi^{0R} \rangle = v_{\text{ew}}$ and all its other components correspond to the GBs eaten by the corresponding gauge bosons. The physical real scalar gets a mass given by

$$m_{h_1}^2 = \frac{2}{3} v_{\text{ew}}^2 (3\lambda_1 + \lambda_3 + \lambda_4 + \lambda_5 \cos\epsilon). \tag{5.16}$$

The neutral components of the other two doublets $\varphi'$ and $\varphi''$ mix into two complex neutral states; their masses are given by

$$m_{n}^{\prime,\prime\prime\,2} = \frac{v_{\text{ew}}^2}{6} \left( -\lambda_3 - \lambda_4 - 4\lambda_5 \cos\epsilon \pm \sqrt{(\lambda_3 + \lambda_4)^2 + 4\lambda_5^2(1 + 2\sin^2\epsilon) - 4(\lambda_3 + \lambda_4)\lambda_5 \cos\epsilon} \right) . \tag{5.17}$$

The charged components of $\varphi', \varphi''$ do not mix; their masses are

$$m_{C}^{\prime,\prime\prime\,2} = -\frac{v_{\text{ew}}^2}{6} \left( 3\lambda_4 + 3\lambda_5 \cos\epsilon \pm \sqrt{3}\lambda_5 \sin\epsilon \right) . \tag{5.18}$$

### 5.6.3 The Alignment $(v, 0, 0)$ when $\epsilon \neq 0$

In the chosen $A_4$ basis, the vacuum alignments $(v, 0, 0)$ preserves the $Z_2$ subgroup of $A_4$. As in the $Z_3$ conserving vacuum, it is useful to rewrite the scalar potential by performing the following $Z_2$ conserving basis transformation

$$\begin{aligned} \Phi_1 &\to \Phi_1 \,, \\ \Phi_2 &\to e^{-i\epsilon/2}\Phi_2 \,, \\ \Phi_3 &\to e^{i\epsilon/2}\Phi_3 \,. \end{aligned} \tag{5.19}$$

$\Phi_1$ is even under $Z_2$ and behaves like the standard Higgs doublet, while $\Phi_2$ and $\Phi_3$ are odd. For what concerns the neutral states, the $6 \times 6$ mass matrix is diagonal in this basis and has some degenerated eigenvalues

$$\begin{aligned} m_{h_1}^2 &\equiv 2\lambda_1 v_{\text{ew}}^2 \,, & m_{h_2}^2 &= m_{h_3}^2 = \frac{1}{2}(\lambda_3 + \lambda_4 - \lambda_5) v_{\text{ew}}^2 \,, \\ m_{h_4}^2 &= m_{h_5}^2 = \frac{1}{2}(\lambda_3 + \lambda_4 + \lambda_5) v_{\text{ew}}^2 \,, & m_{\pi^0}^2 &= 0 \,. \end{aligned} \tag{5.20}$$

[2] In the special case where $\epsilon = 0$, the symmetry of the vacuum is enlarged to $S_3$ even if $S_3$ is not a subgroup of $A_4$. The reason is that setting $\epsilon = 0$ effectively enlarges the symmetry of the potential to $S_4$ (once also $SU(2) \times U(1)$ gauge invariance is required), which does have $S_3$ as a subgroup.

The charged scalar mass matrix is also diagonal with eigenvalues

$$m_{C_1}^2 = m_{C_2}^2 = \frac{1}{2}\lambda_3 v_{\text{ew}}^2\,, \qquad m_{\pi^+}^2 = 0\,. \tag{5.21}$$

The degeneracy in the mass matrices are imposed by the residual $Z_2$ symmetry. Contrary to the previous case the neutral scalar mass eigenstates are real and not complex.

### 5.6.4 The Alignment $(v, v, 0)$ when $\epsilon = 0$

This vacuum alignment does not preserve any subgroup of $A_4$. From the minimum equations we obtain

$$\mu^2 = -\frac{1}{4}v_{\text{ew}}^2(4\lambda_1 + \lambda_3 + \lambda_4 + \lambda_5)\,. \tag{5.22}$$

The scalar and pseudoscalar mass eigenvalues are given by

$$\begin{aligned} m_{h_1}^2 &= -\frac{v_{\text{ew}}^2}{2}(\lambda_3 + \lambda_4 + \lambda_5)\,, & m_{h_2}^2 &= \frac{v_{\text{ew}}^2}{2}(4\lambda_1 + \lambda_3 + \lambda_4 + \lambda_5)\,, \\ m_{h_3}^2 &= \frac{v_{\text{ew}}^2}{4}(\lambda_3 + \lambda_4 + \lambda_5)\,, & m_{h_4}^2 &= -\lambda_5 v_{\text{ew}}^2\,, \\ m_{h_5}^2 &= \frac{v_{\text{ew}}^2}{4}(\lambda_3 + \lambda_4 - 3\lambda_5)\,, & m_{\pi^0}^2 &= 0\,. \end{aligned} \tag{5.23}$$

In the charged sector the masses are given by

$$m_{C_1}^2 = \frac{v_{\text{ew}}^2}{4}(\lambda_3 - \lambda_4 - \lambda_5)\,, \qquad m_{C_2}^2 = -\frac{v_{\text{ew}}^2}{2}(\lambda_4 + \lambda_5)\,, \qquad m_{C_3}^2 = 0\,. \tag{5.24}$$

For $\lambda_5 \neq 0$ the alignment $(v, v, 0)$ has the correct number of GBs, while for $\lambda_5 = 0$ we have an extra massless pseudoscalar. More importantly, the conditions $m_{h_1}^2 > 0$ and $m_{h_3}^2 > 0$ can not be simultaneously satisfied. This alignment is therefore a saddle point of the $A_4$ scalar potential we are studying.

### 5.6.5 The Alignment $(v_1, v_2, v_3)$ when $\epsilon = 0$

This vacuum alignment, as the previous one, does not preserve any subgroup of $A_4$. We recall that this minimum requires two constraints on the parameters of the potential: $\epsilon = 0$ and $\lambda_3 + \lambda_4 + \lambda_5 = 0$.

The mass matrix for the neutral CP-even scalar states has just one massive state

$$m{h_1}^2 = 2\lambda_1 v_{\text{ew}}^2\,. \tag{5.25}$$

There are two additional massless scalars as expected from the enlarged symmetry of the potential. There are two degenerate massive and one massless CP-odd states as well. The massless state is just the Goldstone boson $\pi^0$. The mass of the massive states is

$$m_{h_2}^2 = m_{h_3}^2 = (\lambda_3 + \lambda_4)v_{\text{ew}}^2\,. \tag{5.26}$$

Note that for the special case $\lambda_5 = 0$ even these states are massless as the original symmetry of the potential was even larger. Lastly, for the charged scalars we have

$$m_{C_1}^2 = m_{C_2}^2 = \frac{1}{2}\lambda_3 v_{\text{ew}}^2\,, \qquad m_{C_3}^2 = 0\,. \tag{5.27}$$

The total amount of GBs is 5 (7) for the case $\lambda_5 \neq 0$ ($\lambda_5 = 0$), so we have 2 (4) extra unwanted GBs. We note that the introduction of terms in the potential that softly break $A_4$ can ameliorate the situation with the Goldstone bosons.

### 5.6.6 Analysis of solutions with complex vacua

In the two subsections after this one, we study vacua that are inherently complex. We reiterate that it is always possible to remove one phase by a global rotation. Therefore, it is very easy to give an exhaustive list of vacua: there are just two possibilities.

We order the vacua by the number of zero vevs. Two zeros is not an option, as the only phase in $(v_1 e^{i\omega_1}, 0, 0)$ can always be rotated away. The first possibility is thus the configuration with one zero vacuum expectation value $(v_1 e^{i\omega_1}, v_2, 0)$. A special case occurs if the magnitudes of the two vevs are related. The second possibility reads $(v_1 e^{i\omega_1}, v_2 e^{i\omega_2}, v_3)$ and does not have any zero vevs. A number of special cases is possible, where some or all of the moduli or phases are related. In subsection 5.6.8 we see that the situation with $v_1 = v_2$ and $\omega_1 = -\omega_2$ is of special interest.

We note that the two natural vacua of the previous section $(v, v, v)$ and $(v, 0, 0)$ obviously do not have complex analogues as they have only one phase that can be reabsorbed to make all vevs real. The two less satisfying solutions that appear under the constraint $\epsilon = 0$, given by $(v, v, 0)$ and $(v_1, v_2, v_3)$, do have complex analogues. In the following subsections we show that these are physically more relevant than the real versions.

### 5.6.7 The Alignment $(v_1 e^{i\omega_1}, v_2, 0)$

The third doublet is inert if the Higgs fields appear in the vacuum $(v_1 e^{i\omega_1}, v_2 e^{i\omega_2}, 0)$. We are left only with two doublets that develop a complex vev and after the redefinition, there is only one phase $\omega_1$. Taking the generic solution $(v_1 e^{i\omega_1}, v_2, 0)$ the minimum equations are given by

$$\begin{aligned}
&v_1 \left[\cos\omega_1 [2\mu^2 + 2\lambda_1(v_1^2 + v_2^2) + (\lambda_3 + \lambda_4)v_2^2] + \lambda_5 v_2^2 \cos(\epsilon + \omega_1)\right] = 0\,,\\
&v_2 \left[(2\mu^2 + 2\lambda_1(v_1^2 + v_2^2) + (\lambda_3 + \lambda_4)v_1^2 + \lambda_5 v_1^2 \cos(\epsilon + 2\omega_1)\right] = 0\,,\\
&v_1 \left[\sin\omega_1 [2\mu^2 + 2\lambda_1(v_1^2 + v_2^2) + (\lambda_3 + \lambda_4)v_2^2] - \lambda_5 v_2^2 \sin(\epsilon + \omega_1)\right] = 0\,,\\
&v_2 v_1^2 \sin(\epsilon + 2\omega_1) = 0\,.
\end{aligned} \tag{5.28}$$

The last equation can be solved by $\epsilon = -2\omega_1$ or $\epsilon = -2\omega_1 + \pi$. Like in section 5.6.1, we can absorb the second case by a redefinition of $\lambda_5$. The other three equations reduce to

$$\begin{aligned}
&v_1 \cos\omega_1 \left[2\mu^2 + 2\lambda_1(v_1^2 + v_2^2) + (\lambda_3 + \lambda_4)v_2^2 + \lambda_5 v_2^2\right] = 0\,,\\
&v_2 \left[2\mu^2 + 2\lambda_1(v_1^2 + v_2^2) + (\lambda_3 + \lambda_4)v_1^2 + \lambda_5 v_1^2\right] = 0\,,\\
&v_1 \sin\omega_1 \left[2\mu^2 + 2\lambda_1(v_1^2 + v_2^2) + (\lambda_3 + \lambda_4)v_2^2 + \lambda_5 v_2^2\right] = 0\,.
\end{aligned} \tag{5.29}$$

These equations are simultaneously solved for $v_1 = v_2 = v_{\text{ew}}/\sqrt{2}$ and $\mu^2$ given by

$$\mu^2 = -\frac{v_{\text{ew}}^2}{4}(4\lambda_1 + \lambda_3 + \lambda_4 + \lambda_5)\,. \tag{5.30}$$

The neutral and charged $6 \times 6$ mass matrices can analytically be diagonalized. In the neutral sector we have

$$\begin{aligned}
m_{h_1}^2 &= \frac{1}{2}v_{\text{ew}}^2(-\lambda_3 - \lambda_4 - \lambda_5)\,, & m_{h_2}^2 &= \frac{1}{2}v_{\text{ew}}^2(4\lambda_1 + \lambda_3 + \lambda_4 + \lambda_5)\,,\\
m_{h_3}^2 &= \frac{1}{4}v_{\text{ew}}^2(\lambda_3 + \lambda_4 - \lambda_5 + 2\lambda_5\cos 3\omega_1)\,, & m_{h_4}^2 &= -\lambda_5 v_{\text{ew}}^2\,,\\
m_{h_5}^2 &= \frac{1}{4}v_{\text{ew}}^2(\lambda_3 + \lambda_4 - \lambda_5 - 2\lambda_5\cos 3\omega_1)\,, & m_{\pi^0}^2 &= 0\,.
\end{aligned} \tag{5.31}$$

The charged sector has masses

$$m_{C_1}^2 = \frac{v_{\text{ew}}^2}{4}(\lambda_3 - \lambda_4 - \lambda_5)\,, \qquad m_{C_2}^2 = \frac{v_{\text{ew}}^2}{2}(-\lambda_4 - \lambda_5)\,, \qquad m_{C_3}^2 = 0\,. \tag{5.32}$$

We see that the mass of the fourth neutral boson selects negative values for $\lambda_5$, i.e. the second solution $\epsilon = -2\omega_1 + \pi$. It is interesting to see that in the real limits $\omega_1 \to 0$ (or $\pi$), it is not possible to have both $m^2_{h_1}$ and $m^2_{h_3}$ (respectively $m^2_{h_5}$) positive. This was indeed the conclusion of subsection 5.6.4. Only in the complex situation, there are points in parameter space where all masses are positive. This is in particular clear in the region around $\cos 3\,\omega_1 = 0$. As before, $\lambda_5 = 0$ leads to two problems: an extra GB and impossibility to have all massive eigenstates positive.

### 5.6.8 The Alignment $(v_1 e^{i\omega_1}, v_2 e^{i\omega_2}, v_3)$

We now consider the alignment where all Higgs doublets develop a non-zero vev. This leads to two physical phases. We have the freedom to take $\omega_3 = 0$. In this case the first-derivative system is given by

$$\begin{aligned}
&v_1 \left\{\cos\omega_1[2\mu^2 + 2\lambda_1(v_1^2+v_2^2+v_3^2) + (\lambda_3+\lambda_4)(v_2^2+v_3^2)] + \right. \\
&\qquad \left. +\lambda_5[v_3^2\cos(\epsilon-\omega_1) + v_2^2\cos(\epsilon+\omega_1-2\omega_2)]\right\} = 0\,, \\
&v_2 \left\{\cos\omega_2(2\mu^2 + 2\lambda_1(v_1^2+v_2^2+v_3^2) + (\lambda_3+\lambda_4)(v_1^2+v_3^2) + \right. \\
&\qquad \left. +\lambda_5[v_3^2\cos(\epsilon+\omega_2) + v_1^2\cos(\epsilon-\omega_2+2\omega_1)]\right\} = 0\,, \\
&v_3 \left\{2\mu^2 + 2\lambda_1(v_1^2+v_2^2+v_3^2) + (\lambda_3+\lambda_4)(v_1^2+v_2^2) + \right. \\
&\qquad \left. +\lambda_5[v_1^2\cos(\epsilon-2\omega_1) + v_2^2\cos(\epsilon+2\omega_2)]\right\} = 0\,, \\
&v_1 \left\{\sin\omega_1[2\mu^2 + 2\lambda_1(v_1^2+v_2^2+v_3^2) + (\lambda_3+\lambda_4)(v_2^2+v_3^2)] + \right. \\
&\qquad \left. +\lambda_5[v_3^2\sin(\epsilon-\omega_1) - v_2^2\sin(\epsilon+\omega_1-2\omega_2)]\right\} = 0\,, \\
&v_2 \left\{\sin\omega_2(2\mu^2 + 2\lambda_1(v_1^2+v_2^2+v_3^2) + (\lambda_3+\lambda_4)(v_1^2+v_3^2)) + \right. \\
&\qquad \left. +\lambda_5[-v_3^2\sin(\epsilon+\omega_2) + v_1^2\sin(\epsilon-\omega_2+2\omega_1)]\right\} = 0\,, \\
&v_3 \left[\lambda_5(-v_1^2\sin(\epsilon-2\omega_1) + v_2^2\sin(\epsilon+2\omega_2))\right] = 0\,.
\end{aligned} \tag{5.33}$$

The last equation is solved for $\omega_2 = -\omega_1$ and $v_2 = v_1 = v$. We have checked explicitly that this is the only solution for the last equation that is compatible with the other equations. Defining $v_3 = rv$ and $v_1^2 + v_2^2 + v_3^2 = v_{\text{ew}}^2$ the previous system reduces to three equations

$$\begin{aligned}
&\mu^2 + \frac{v_{\text{ew}}^2}{2(2+r^2)}\left[(4+2r^2)\lambda_1 + (1+r^2)(\lambda_3+\lambda_4) + \frac{\lambda_5}{\cos\omega_1}(r^2\cos(\epsilon-\omega_1) + \cos(\epsilon+3\omega_1))\right] = 0\,, \\
&\mu^2 + \frac{v_{\text{ew}}^2}{2(2+r^2)}\left[(4+2r^2)\lambda_1 + (1+r^2)(\lambda_3+\lambda_4) + \frac{\lambda_5}{\sin\omega_1}(r^2\sin(\epsilon-\omega_1) + \sin(\epsilon+3\omega_1))\right] = 0\,, \\
&\mu^2 + \frac{v_{\text{ew}}^2}{(2+r^2)}\Big[(2+r^2)\lambda_1 + \lambda_3 + \lambda_4 + \lambda_5\cos(\epsilon-2\omega_1)\Big] = 0\,.
\end{aligned} \tag{5.34}$$

We can solve the third equation in (5.34) in terms of $\mu^2$. Thereafter, the second equation can be solved in terms of $\lambda_5$.

$$\begin{aligned}
\mu^2 &= -\tfrac{v_{\text{ew}}^2}{2+r^2}[(2+r^2)\lambda_1 + \lambda_3 + \lambda_4 + \lambda_5\cos(\epsilon-2\omega_1)]\,, \\
\lambda_5 &= \frac{(r^2-1)(\lambda_3+\lambda_4)\sin\omega_1}{(r^2-1)\sin(\epsilon-\omega_1) - 2\cos\epsilon\sin(3\omega_1)}\,.
\end{aligned} \tag{5.35}$$

Then the first equation in (5.34) has two possible solutions, for $\lambda_4$ and $\epsilon$ respectively

$$\begin{aligned}
&i) \quad \lambda_4 = -\lambda_3\,, \\
&ii) \quad \tan\epsilon = \frac{r^2\sin 2\omega_1 + \sin 4\omega_1}{r^2\cos 2\omega_1 - \cos 4\omega_1}\,.
\end{aligned} \tag{5.36}$$

The solutions (5.35) and (5.36) seem to constrain the potential severely, fixing three of the potential parameters in a non-trivial way. This is indeed true for solution i) in (5.36), but in the other case the potential is still completely general; we have just expressed three of its parameters ($\mu^2$, $\lambda_5$ and $\epsilon$) in terms of parameters of the vev system ($v_{\text{ew}}$, $r$ and $\omega_1$).

To test the validity of the solution so far sketched it is necessary to check whether this is a true minimum of the potential and furthermore if there are extra GBs apart from three corresponding to electroweak symmetry breaking. Unfortunately the relations given in (5.35) and (5.36) do not allow

to get analytical solutions for the scalar masses in case $ii)$. For this reason we consider only three special limits in this case : $r \sim 0$, $r \sim 1$ and $r$ very large. We think that these limit situations could be the most interesting ones in model building realizations. Indeed two of the models [127,128] that we discuss in section 5.10 and test in section 5.12 use this vacuum with a large value of $r$, respectively 43 and 240.

**Case** $i)$

In this case the constrains $\lambda_4 = -\lambda_3$ puts $\lambda_5$ to zero and this substantially enlarges the symmetries of the potential. There is an accidental $O(3)$ in the neutral real direction and two accidental $U(1)$s due to $\lambda_5 = 0$. For this reason the neutral spectrum has 5 massless particles, the GB $\pi^0$ and 4 other GBs, and only one massive state

$$m_{h_1}^2 = 2\lambda_1 v_{\rm ew}^2 \,. \tag{5.37}$$

The charged scalars are

$$m_{C_1}^2 = m_{C_2}^2 = \frac{1}{2}\lambda_3 v_{\rm ew}^2 \,, \qquad\qquad m_{C3}^2 = 0 \tag{5.38}$$

**Case** $ii)$

In this case, it is unfortunately not possible to find analytical solutions. Instead we consider three situations where $r$ takes special values: $r \ll 1$ (in numerical examples $r \sim 0.05$); $r \sim 1$ and $r \gg 1$ (where we take $r$ in the range $50 \div 200$ in numerical studies). See also figure 5.1.

In all these three cases, we find the appearance of very light states. This does obviously not prove that light states are a necessary consequence of case ii) of the $(ve^{i\omega_1},\ ve^{-i\omega_1},\ rv)$ vacuum, but it is a rather strong hint that the vacuum is, at least to some degree, pathological. The problem of the light states can be alleviated by introducing soft $A_4$ breaking terms. Indeed we opt to add these terms to the models studied in section 5.10.


Figure 5.1: *The three ranges of $r$ studied in this subsection.*

- $r \sim 0$

In this case we assume that $r$ is small and that we can thus neglect terms of order $r^2$. Equation (5.36) is easily solved for $\epsilon$

$$\epsilon \sim -4\omega_1 + N\pi \,. \tag{5.39}$$

Inserting these values in the equations of (5.35) we find

$$\begin{aligned} \mu^2 &= -\lambda_1 v_{\rm ew}^2 - (\lambda_3 + \lambda_4)\frac{1 - \cos 6\omega_1}{2 - 4\cos 6\omega_1} \,, \\ \lambda_5 &= \frac{\lambda_3 + \lambda_4}{1 - 2\cos 6\omega_1} \,. \end{aligned} \tag{5.40}$$

Under these approximations the 6 x 6 neutral scalar mass matrix gives one massless state, $m_{\pi^0}^2 = 0$,

corresponding to the GB. The other five eigenvalues are at leading order in $r$ given by

$$\begin{aligned}
m_{h_1}^2 &\sim f[\lambda_i]\mathcal{O}(r^2)v_{\rm ew}^2 \\
m_{h_2}^2 &\sim -(\lambda_3+\lambda_4)/(1-2\cos 6\omega_1)v_{\rm ew}^2 \\
m_{h_3}^2 &\sim [-2\lambda_1+(4\lambda_1+\lambda_3+\lambda_4)(1-\cos 6\omega_1)/(1-2\cos 6\omega_1)]\, v_{\rm ew}^2 \\
m_{h_4}^2 &\sim -\left[(\lambda_3+\lambda_4)\cos 6\omega_1 v_w^2/(1-2\cos 6\omega_1)\right] v_{\rm ew}^2\,, \\
m_{h_5}^2 &\sim -\left[2(\lambda_3+\lambda_4)\sin^2 3\omega_1/(1-2\cos 6\omega_1)\right] v_{\rm ew}^2\,.
\end{aligned} \tag{5.41}$$

Here $f[\lambda_i]$ stands for a linear combination of the dimensionless $\lambda$ parameters of the potential. The lightest state in (5.41) may be too light to be phenomenologically acceptable. We estimate its mass by choosing $f[\lambda_i]$ in the range $0.1 \div 10$ (natural values for a function of dimensionless parameters) or $10^{-2} \div 10^2$ (slightly unnatural). Reference values for $r^2$ are $10^{-3} \div 10^{-2}$. Under these conditions, we find upper bounds

$$\begin{aligned}
m_{h_1}^2 &\leq 200\,{\rm GeV}^2 \qquad \text{for} \quad \lambda_i \sim 100, r^2 \sim 10^{-2}\,, \\
m_{h_1}^2 &\leq 25\,{\rm GeV}^2 \qquad \text{for} \quad \lambda_i \sim 10, r^2 \sim 10^{-3}\,.
\end{aligned} \tag{5.42}$$

This indicates that for small value of $r$ the spectrum is likely to contain very light neutral states. On the contrary, in the charged sector we have the two GBs eaten by the corresponding gauge bosons, $m_{C_3}^2 = 0$, and two states that are not very light.

$$\begin{aligned}
m_{C_1}^2 &\sim -[\lambda_4 + (\lambda_3+\lambda_4\cos 6\omega_1)/(1-2\cos 6\omega_1)]v_{\rm ew}^2/2 \\
m_{C_2}^2 &\sim -[2\lambda_4 + (\lambda_3+2\lambda_4\cos 6\omega_1)/(1-2\cos 6\omega_1)]v_{\rm ew}^2/2\,.
\end{aligned} \tag{5.43}$$

- $r \sim 1$

If $r$ is close to 1, we write $r \sim 1+\delta$ and make an expansion in terms of $\delta$, neglecting terms of order $\delta^2$. This gives for $\epsilon$

$$\epsilon \sim \pi/2 - \omega_1 - \delta\cot 3\omega_1 + N\pi\,. \tag{5.44}$$

Equations (5.35) for $\mu^2$ and $\lambda_5$ become

$$\begin{aligned}
\mu^2 &= -(3\lambda_1+\lambda_3+\lambda_4)/3v_{\rm ew}^2 - \delta/9(\lambda_3+\lambda_4)v_{\rm ew}^2\,, \\
\lambda_5 &= \delta(\lambda_3+\lambda_4)\csc 3\omega_1\,.
\end{aligned} \tag{5.45}$$

Under these approximations the 6 x 6 neutral scalar mass matrix gives the usual null mass state, $m_{\pi^0}^2 = 0$, corresponding to the GB and the following five eigenvalues

$$\begin{aligned}
m_{h_1}^2 &\sim m_{h_2}^2 \sim f[\lambda_i]\mathcal{O}(\delta^2)v_{\rm ew}^2\,, \\
m_{h_3}^2 &\sim m_{h_4}^2 \sim -(\lambda_3+\lambda_4)/3v_{\rm ew}^2\,, \\
m_{h_5}^2 &\sim 2(3\lambda_1+\lambda_3+\lambda_4)/3v_{\rm ew}^2\,,
\end{aligned} \tag{5.46}$$

Again $f[\lambda_i]$ stays for a linear combination of the $\lambda$s. An analysis similar to the one for the case with $r \sim 0$ shows that the neutral spectrum typically has very light states.

In the charged sector we have the GBs eaten by the gauge bosons and two degenerate massive states

$$m_{C_1}^2 \sim m_{C_2}^2 \sim -\lambda_4/2v_{\rm ew}^2\,. \tag{5.47}$$

- $r \gg 1$

In the situation where $r$ is large, we perform an expansion in term of $1/r$ and neglect terms of order $1/r^2$. From equation (5.36) we find

$$\epsilon \sim 2\omega_1 + N\pi\,. \tag{5.48}$$

After this, equation (5.35) reduces to

$$\mu^2 \sim -\lambda_1 v_{\text{ew}}^2 \,, \tag{5.49}$$
$$\lambda_5 \sim -(\lambda_3+\lambda_4)\,. \tag{5.50}$$

Under these approximations we find a massless neutral scalar state, $m_{\pi^0}^2 = 0$. The other 5 neutral masses are given at leading order by

$$\begin{aligned} m_{h_1}^2 &\sim m_{h_2}^2 \sim f[\lambda_i]\mathcal{O}(1/r^2) v_{\text{ew}}^2 \,, \\ m_{h_3}^2 &\sim 2\lambda_1 v_{\text{ew}}^2 \,, \\ m_{h_4}^2 &\sim m_{h_5}^2 \sim (\lambda_3+\lambda_4) v_{\text{ew}}^2 \,. \end{aligned} \tag{5.51}$$

The charged scalar mass matrix is diagonal up to terms of order $\mathcal{O}(1/r^2)$ with the correct number of GBs and two massive degenerate states

$$m_{C_1}^2 = m_{C_2}^2 = \lambda_3 v_{\text{ew}}^2/2\,. \tag{5.52}$$

From equation (5.51) it follows that again there are two very light neutral scalars. Using reference values for $r$ in the range $50 \div 200$ we find

$$m_{h_{1,2}}^2 \sim \sqrt{f[\lambda_i]}\,5\,\text{GeV}^2(1\,\text{GeV}^2)\,. \tag{5.53}$$

For 'small' values of $f[\lambda_i]$ as defined above, the minimal masses that this expression can reproduce are

$$\begin{aligned} m_{1,2}^2 &\leq 50^2 \quad \text{GeV}^2 \quad \text{for} \quad r \sim 50\,, \\ m_{1,2}^2 &\leq 10^2 \quad \text{GeV}^2 \quad \text{for} \quad r \sim 200\,. \end{aligned} \tag{5.54}$$

Again we find that naturally very light scalars appear. In conclusion the solution $(e^{i\omega_1}, e^{-i\omega_1}, r)v_{\text{ew}}/\sqrt{2+r^2}$ gives very light states in each of the domains for $r$ investigated, at least under the assumption that the functions $f[\lambda_i]$ obtained somewhat natural values. We reiterate that this is no formal proof that there exist light states for all values of $r$.

### 5.6.9 List of the available minima

In this section we have scanned the possible solutions of the first derivative system (5.8) of the $A_4$-invariant Higgs potential (5.4). Three candidate-vacua seemed to be under control.

- The vacuum $(v,\, v,\, v)$ of section 5.6.2.
- The vacuum $(v,\, 0,\, 0)$ of section 5.6.3.
- The vacuum $(ve^{i\omega_1}, v, 0)$ of section 5.6.7. We note that the global rotation used to get rid of the second phase could equally well be used to give the first two elements equal but opposite phases: $(ve^{i\omega_1/2}, ve^{-i\omega_1/2}, 0)$

These configurations have the right number of Goldstone bosons and in a large part of parameter space all masses are positive and in a reasonable range.

Two vacua were more problematic

- The alignment $(v_1,\, v_2,\, v_3)$ of section 5.6.5.
- The alignment $(v\, e^{i\omega_1},\, v\, e^{-i\omega_1},\, r\, v)$ of section 5.6.8.

The first vacuum here was derived under the assumption of non-trivial relations of parameters in the potential. As a result, obtaining this vacuum implies breaking extra symmetries next to electroweak symmetry. The second vacuum has two realizations, case i) and case ii). The first case suffers from the same handicaps as the previous vacuum: the potential parameters are related and extra symmetries gets broken when the Higgses develop vacuum expectation values. The second case technically gives a correct vacuum. However, for all values of $f[\lambda_i]$ and $r$ studied, very light states appeared. In all situations, a solution is to add soft $A_4$ breaking terms to the potential, although that significantly reduces the appeal of the method. Lastly, one of the solutions, the candidate-vacuum $(v,\, v,\, 0)$ of section 5.6.4 turned out to be always a saddle point and is not discussed further.

## 5.7 Discussion on CP violation

The $A_4$-invariant Higgs potential 5.4 central in this chapter has an explicit complex phase $\epsilon$. Furthermore, the solutions studied in sections 5.6.7 and 5.6.8 had an explicit complex phase $\omega_1$ in some of the vacuum expectation values. One might thus wonder whether the Higgs sector in $A_4$ models gives rise to extra sources of CP violation. This CP violation can be either explicit if it appears directly at the level of the Higgs potential or implicit if it occurs due to the vacuum expectation values of the scalars. In this section we investigate explicit and implicit CP violation in the $A_4$ Higgs scenario. The conclusion is that neither is present. This section owes to [129] in which the question of CP violation in our class of models was first discussed in detail.

We first investigate if the potential 5.4 exhibits explicit CP violation. We find that the potential is not invariant under a 'naive' CP transformation

$$\Phi_i \xrightarrow{\text{CP}} \Phi_i^* \,, \qquad \text{i.e. } \Phi_i \xrightarrow{\text{CP}} \delta_{ij}\Phi_j^* \,. \tag{5.55}$$

Under this transformation $\epsilon$ and $-\epsilon$ get interchanged in the potential (5.4). Equation (5.55) does not describe the most general CP transformation however. A more general CP transformation follows when the 'pure' CP transformation (5.55) is combined with a Higgs basis transformation

$$\Phi_i \xrightarrow{\text{CP}} U_{ij}\Phi_j^* \,. \tag{5.56}$$

Here $U$ is a unitary matrix in the space of the three Higgs fields. It was shown in [130] that the Higgs potential conserves CP explicitly if a matrix $U$ exists such that the 'new' CP transformation (5.56) leaves the potential invariant. For the potential (5.4) it is not hard to find such a matrix. An example is the matrix that parameterizes the interchange of the first and second Higgs field

$$U = \begin{pmatrix} 0 & 1 & 0 \\ 1 & 0 & 0 \\ 0 & 0 & 1 \end{pmatrix} \,. \tag{5.57}$$

In this case, the CP transformation is defined according to

$$\Phi_1 \xrightarrow{\text{CP}} \Phi_2^*, \quad \Phi_2 \xrightarrow{\text{CP}} \Phi_1^*, \quad \Phi_3 \xrightarrow{\text{CP}} \Phi_3^* \,. \tag{5.58}$$

We conclude that the $A_4$ invariant Higgs potential does not violate CP explicitly. There is still the possibility of spontaneous CP violation through the complex vacua discussed in the previous section. In [130] and [131] it is shown that a vacuum does not give rise to spontaneous CP violation if there is a matrix $U$ such that the CP transformation (5.56) also leaves the vacuum invariant. In that case, the vacuum thus satisfies

$$(vac) = U\ (vac)^* \,. \tag{5.59}$$

In other words, each component $v_i e^{i\omega_i}$ of the vector of vevs should be written as a linear combination of the complex conjugates of the vevs $v_j e^{i\omega_j}$ with the coefficients given by $U_{ij}$

$$v_i e^{i\omega_i} = U_{ij} v_j\ e^{-i\omega_j} \,. \tag{5.60}$$

In the specific case under investigation, where $U$ has the form (5.57), this is represented by

$$v_1 e^{i\omega_1} = v_2 e^{-i\omega_2}, \quad v_2 e^{i\omega_2} = v_1 e^{-i\omega_1}, \quad v_3 e^{i\omega_3} = v_3 e^{-i\omega_3} \ . \tag{5.61}$$

The first two equations are dependent; they require $v_1$ and $v_2$ to be each others complex conjugate. The third equation requires the third vev to be real. The two candidate-CP-violating vacua, $(ve^{i\omega_1/2},\ ve^{-i\omega_1/2},\ 0)$ and $(v\,e^{i\omega_1},\, v\,e^{-i\omega_1},\, r\,v)$ both satisfy the conditions (5.61). They do thus not break CP spontaneously, notwithstanding the fact that they are inherently complex[3].

The criterium of conserving or violating CP depending on whether the transformation matrix $U$ exists, is not always a very practical one. Even if such a transformation exists, it may not be easy to find. A more solid test is in the calculation of CP-odd basis invariants that vanish if CP is conserved and that are non-zero if CP is violated (or, at least one of them is). Invariants for the potential (5.4) and the vacua of the previous subsection were calculated in [129]. As expected, they are all zero.

## 5.8 Description of model-independent tests of the viability of vacua

The most direct tests for the scenario of this chapter, is obviously the direct detection of the extended Higgs sector. In each of the vacua of section 5.6 we mentioned the appearance of multiple Higgs bosons with specific relations between their masses. The LHC recently cut deep into the parameter space available to the Standard Model Higgs boson, excluding much of its mass range and finding hints for a Higgs around 125 GeV, see for instance [132,133]. Bounds for non-Standard Model Higgses have also been obtained. We have not yet applied these bounds to our model. The fact that the data are not sufficient to exclude slightly similar multi-Higgs scenarios, in particular the MSSM, however hints to the statement that more data will be needed to test our model via direct detection of the Higgs fields involved.

In this section we analyze three more indirect tests for the vacuum configurations derived in section 5.6. These tests only require pre-LHC data and involve phenomenology of the Higgs sector only. As such they are model independent according to the definition of section 5.3 as the $A_4$ representations of the various fermions in the theory need not be fixed.

The three tests are unitarity; $Z$ and $W^\pm$ decays and oblique parameters. In the next section we use these three tests to examine the viability of the vacua of section 5.6 and to restrict their parameter space.

### 5.8.1 Unitarity

A first test for multi-Higgs models comes from the tree level unitarity constraints due to the additional scalars present in the theory. In this subsection, we examine the partial wave unitarity for the neutral two-particle amplitudes for $s \gg M_W^2, M_Z^2$. We can use the equivalence theorem, so that we can compute the amplitudes using only the scalar potential given in (5.4). In the regime of large energies, the only relevant contributions are the quartic couplings in the scalar potential [134–137] and we can write the $J = 0$ partial wave amplitude $a_0$ in terms of the tree level amplitude $T$ as

$$a_0(s) \equiv \frac{1}{32\pi} \int_{-1}^{1} \mathrm{d}\cos\theta \; T(s) = \frac{1}{16\pi} F[\lambda_i] \, . \tag{5.62}$$

[3]We recall that via a global rotation the first complex vacuum can also be written as $(ve^{i\omega_1},\ v,\ 0)$ and it was indeed derived in this form in section 5.6.7. In this case, $U$ should contain a phase as well and is written as $e^{i\omega_1}$ times the matrix in equation (5.57).

Here $F$ represents a function of the $\lambda_i$ couplings. For simplicity we use the notation

$$\Phi_a = \begin{pmatrix} w_a^+ \\ \dfrac{v_a e^{i\omega_a} + h_a^0 + i z_a}{\sqrt{2}} \end{pmatrix} . \tag{5.63}$$

Now we can write the 30 neutral two-particle channels as follows:

$$w_a^+ w_b^- \,,\ \frac{z_a z_b}{\sqrt{2}} \,,\ \frac{h_a^0 h_b^0}{\sqrt{2}} \,,\ h_a^0 z_b \,. \tag{5.64}$$

The full scattering matrix $a_0$ can be cast in a block diagonal structure. The first $12 \times 12$ block concerns the channels

$$w_1^+ w_1^- \,,\ w_2^+ w_2^- \,,\ w_3^+ w_3^- \,,\ \frac{z_1 z_1}{\sqrt{2}} \,,\ \frac{z_2 z_2}{\sqrt{2}} \,,\ \frac{z_3 z_3}{\sqrt{2}} \,,\ \frac{h_1^0 h_1^0}{\sqrt{2}} \,,\ \frac{h_2^0, h_2^0}{\sqrt{2}} \,,\ \frac{h_3^0, h_3^0}{\sqrt{2}} \,,\ h_1^0 z_1 \,,\ h_2^0 z_2 \,,\ h_3^0 z_3 \,.$$

The other three $6 \times 6$ blocks are related to six channels parameterized by the labels $(a,\, b)$ that take values $(1,\, 2)$, $(1,\, 3)$ and $(2,\, 3)$:

$$w_a^+ w_b^- \,,\ w_b^+ w_a^- \,,\ h_a^0 z_b \,,\ h_b^0 z_a \,,\ z_a z_b \,,\ h_a^0 h_b^0 \,,$$

Note that up this point the analysis is completely general and is valid for all the vacua presented. When testing a vacuum configuration, we express the quartic couplings $\lambda_i$ in terms of the masses of the scalars. Afterwards, we can use the constraint that the largest eigenvalues of the scattering matrix $a_0$ has modulus less than 1. This gives upper bounds on the scalar masses that we can use in a numerical analysis.

### 5.8.2 $Z$ And $W^\pm$ Decays

The next test we perform is related to the decay of $Z$ and $W$ gauge bosons. From an experimental point of view the decay of gauge bosons into scalar particles is detected by looking at fermionic channels, such as $Z \to hA \to 4f$ in the 2HDM, or $Z$ decays into partial or total missing energy in a generic new physics scenario. From this point of view gauge bosons decays bound the Higgs sector in an extremely model dependent way as they are highly sensitive to the fermion content of the theory.

On the other hand, in the SM the $Z$ and the $W^\pm$ decays have precisely been calculated and measured not only for decay into 2 or 4 fermions, but also for the sum of all decays. We can thus focus on the decays $Z, W^\pm \to all$. Doing this we overestimate the allowed regions in the parameter space, but we have a first and model-independent cut arising from the decay of the gauge bosons. Once we pass to a model dependent analysis the region can only be restricted, not enlarged. Actually, we expect the error to be quite small, given that the contribution from new physics $\Delta\Gamma$ satisfies

$$\Delta\Gamma^{2f}_{Z,W^\pm} \sim \Delta\Gamma^{4f}_{Z,W^\pm} \sim \Delta\Gamma^{all}_{Z,W^\pm} \ll \Gamma_{Z,W^\pm} \,. \tag{5.65}$$

LEP data give an estimate for the width that can be assigned to new physics effects

$$\Gamma^{\text{exp}}_{Z,W^\pm} = \Gamma^{\text{SM}}_{Z,W^\pm} + \Delta\Gamma_{Z,W^\pm} \,. \tag{5.66}$$

Experimentally $\Delta\Gamma_Z \sim 0.0023$ GeV and $\Delta\Gamma_{W^\pm} \sim 0.042$ GeV [6]. This can be used to calculate the width of $Z$ and $W$ decay to respectively two neutral Higgs states and to one neutral and one charged state.

$$\begin{aligned} Z &\to h_i h_j \,, \\ W^+ &\to h_i^+ h_j \,. \end{aligned} \tag{5.67}$$

In the final step we select the points for which the the widths of the $Z$ and $W$ bosons due to the multi-Higgs set up are allowed by the LEP data.

$$\Gamma^{\rm MH}_{Z,W^\pm} \leq \Delta\Gamma_{Z,W^\pm} \,. \tag{5.68}$$

In the vacuum analysis of section 5.6 we have seen that in a few situations there are extra massless or very light particles. Even if we assume that these do not directly rule out the related configurations (some light scalars may indeed be hard to find directly), the gauge-boson decays put very strong bounds on their existence. Bound on $Z$ decay translate to the following inequalities

$$\begin{cases} k_Z \leq \Delta\Gamma_Z \dfrac{16\pi}{m_Z}\dfrac{4c_W^2}{g^2} & \text{if both particles } h_i \text{ and } h_j \text{ are massless}\,. \\ k_Z \left(1-\dfrac{m_{h_i}^2}{m_Z^2}\right)^3 \leq \Delta\Gamma_Z \dfrac{16\pi}{m_Z}\dfrac{4c_W^2}{g^2} & \text{if } h_j \text{ is massless and } 0<m_{h_i}^2<m_Z^2\,. \\ k_Z \left(1-\dfrac{m_{h_i}^2+m_{h_j}^2}{m_Z^2}\right)^3 \leq \Delta\Gamma_Z \dfrac{16\pi}{m_Z}\dfrac{4c_W^2}{g^2} & \text{if } h_i,h_j\neq 0 \text{ and } 0<m_{h_i}^2+m_{h_j}^2<m_Z^2\,. \end{cases} \tag{5.69}$$

In these equations, $g$ is the $SU(2)$ gauge coupling, $c_W$ the cosine of the Weinberg angle $\theta_W$ and the parameter $k_Z$ is expressed in terms of the matrix $U$ defined in equation (5.6)

$$k_Z = \left(-U^T_{ab}U^T_{(a+3)c} + U^T_{(a+3)b}U^T_{ac}\right)^2 \,. \tag{5.70}$$

A similar equation exist for $W^\pm$ decay in the situation where $h_j$ is massless and $m_{C_i}^2 < m_W^2$

$$k_W \left(1-\frac{m_{C_i}^2}{m_W^2}\right)^3 \leq \Delta\Gamma_W \frac{16\pi}{m_W}\frac{4c_W}{g^2} \,. \tag{5.71}$$

Analogous to $k_Z$, the parameter $k_W$ is given in terms of the matrix $S$ defined in equation (5.7).

$$k_W = \left|S^\dagger_{ab}U^T_{ac}\right|^2 + \left|S^\dagger_{(a+3)b}U^T_{(a+3)c}\right|^2 \,. \tag{5.72}$$

**Large Mass Higgs Decay**

Electroweak data analysis considering the data from LEP2 [138] and Tevatron [139] put an upper bound on the mass of the SM Higgs of 194 GeV at 99% CL [6]. In a MH scenario this bound can be roughly translated in the upper bound for the lightest scalar mass, $m_{h_1}$. For large values of the SM Higgs mass, $m_h \geq 2m_W$, the main decay is $h \to W^+W^-$ and the upper bound is completely 'model independent' in the sense that it does not depend on the fermionic content of the model.

In a MH model the lightest Higgs boson coupling to the gauge bosons is given in terms of a parameter $\beta \leq 1$

$$\begin{aligned} g_{h_1ZZ} &= \beta\, g^{SM}_{hZZ}\,, \\ g_{h_1WW} &= \beta\, g^{SM}_{hWW}\,. \end{aligned} \tag{5.73}$$

In the three-Higgs model, $\beta$ is given by

$$\beta = \frac{v_a}{v_{\rm ew}} f_a(\cos\omega_a\, U^T_{a1} + \sin\omega_j\, U^T_{(a+3)1})\,. \tag{5.74}$$

In these models, the lightest Higgs $h_1$ is less copiously produced than the SM Higgs of the same mass, which in turn is always less than the SM Higgs production at the highest allowed mass of 194 GeV

$$\Gamma^{MH}_{WW}(m_{h_1}) \sim |\beta|^4 \Gamma^{SM}_{WW}(m_{h_1}) \leq \Gamma^{SM}_{WW}(194)\,. \tag{5.75}$$

We use this to obtain an upper bound for $m_{h_1}$ of 194 GeV.

### 5.8.3 Constraints By Oblique Corrections

Lastly, the consistency of a MH model with the current experimental data has to be checked also by means of the oblique corrections. These corrections can be classified [140–145] by means of three parameters, $S$ $T$ and $U$, that maybe written in terms of the physical gauge-boson vacuum polarizations

$$\begin{aligned} T &= \frac{4\pi}{e^2 c_W^2 m_Z^2}\left[A_{WW}(0) - c_W^2 A_{ZZ}(0)\right] , \\ S &= 16\pi \frac{s_W^2 c_W^2}{e^2}\left[\frac{A_{ZZ}(m_Z^2) - A_{ZZ}(0)}{m_Z^2} - A'_{\gamma\gamma}(0) - \frac{(c_W^2 - s_W^2)}{c_W s_W} A'_{\gamma Z}(0)\right] , \\ U &= -16\pi \frac{s_W^2}{e^2}\left[\frac{A_{WW}(m_W^2) - A_{WW}(0)}{m_W^2} - c_W^2 \frac{A_{ZZ}(m_Z^2) - A_{ZZ}(0)}{m_Z^2} - s_W^2 A'_{\gamma\gamma}(0) - 2 s_W c_W A'_{\gamma Z}(0)\right] . \end{aligned} \tag{5.76}$$

As in equation (5.69), $c_W$ is the cosine of $\theta_W$ and $s_W$ is its sine; $e$ is the electric charge. EW precision measurements severely constrain the possible values of the three parameters $T$, $S$ and $U$. In the SM assuming $m_h^2 > m_Z^2$ the oblique parameters are given by

$$\begin{aligned} T_h^{SM} &\sim -\frac{3}{16\pi c_W^2}\log\frac{m_h^2}{m_Z^2} , \\ S_h^{SM} &\sim \frac{1}{12\pi}\log\frac{m_h^2}{m_Z^2} , \\ U_h^{SM} &\sim 0 . \end{aligned} \tag{5.77}$$

For a Higgs boson mass of $m_h = 117$ GeV (and in brackets the difference assuming instead $m_h = 300$ GeV), the data allow [6]

$$\begin{aligned} S^{exp} &= 0.10 \pm 0.10(-0.08) \\ T^{exp} &= 0.03 \pm 0.11(+0.09) \\ U^{exp} &= 0.06 \pm 0.10(+0.01) . \end{aligned} \tag{5.78}$$

A detailed analysis on the $S$, $T$ and $U$ parameters in a MH model has been presented in [146, 147] where all details are carefully explained. However the resulting formulas are valid only for scalar masses larger or comparable to $m_Z$. This is not the case for a generic MH model. In particular in some of the configurations studied in the previous section there are massless and extremely light particles. We modify their results, getting full formulas valid for any value of the scalar masses in appendix 5.A.

## 5.9 Results of the model-independent tests

In this section we report on numerical analyses for all vacuum configurations summarized in section 5.6.9. The aim of the analysis is to find, for each configuration, whether a region in parameter space exists, where all the Higgs constraints are satisfied. Points in parameter space are generated and then tested through subsequent constraints, from the weaker one to the strongest. Points that 'pass' a certain test and then 'fail' the next one are classified as points Y, B and G. Points that 'pass' all tests are referred to as R.

- Points Y. These points are true minima: all the squared masses are positive, but the unitarity test fails (yellow points in the figures);
- Points B. These points are true minima and the unitarity bounds are passed, but $Z$ and $W^\pm$ decays are not (blue points);

- Points G. Here also the $Z$ and $W^{\pm}$ decays are according to data, but the oblique parameters are not (green points);
- Points R. These points pass all tests we performed, including being in accordance with the $T$, $S$ and $U$ parameters (red points).

The ratios $B/Y$, $G/B$, $R/G$ can be used to indicate which is the stronger constraint for each of the allowed minima. Whenever possible, we plot the mass of the lightest neutral state $m_1$ to the mass of the second lightest neutral state $m_2$ and of the lightest charged one $m_{ch_1}$. For all green points that pass the unitarity and $W/Z$ constraints, i.e. the green and the red points, we plot the $T$ and $S$ oblique parameters. It turns out that for all cases considered that $T$ is the most constraining one. For this reason we have not inserted the plots concerning $U$.

### 5.9.1 The Alignment $(v, v, v)$

We first consider the minimum $(v, v, v)$. We showed in section 5.6.2 that this conserves a $Z_3$ symmetry. There we have also redefined the initial 3 doublets in terms of the surviving $Z_3$ symmetry representations: $1$, $1'$ and $1''$. One combination corresponds to a $Z_3$ singlet doublet, that behaves like the SM Higgs: it develops a non-vanishing vev, gives rise to a CP even state which we call $h_1$ and to the three GBs eaten by the gauge bosons. The others two doublets, $\varphi'$ and $\varphi''$, are inert. Depending on which Higgs is the lightest, we can describe the allowed decay patterns and describe what is expect from a numerical scan. The results of this scan are given in figure 5.2.

1) When $h_1$ is the lightest state, the usual SM mass upper bound applies. On the contrary as long as we do not consider its coupling with the fermions we do not have a model-independent lower mass bound. This is due to a combined effect of the CP and $Z_3$ symmetries: $h_1$ is CP even and a singlet under $Z_3$. This forbids couplings like $Zh_1h_1$, $Zh_1\varphi'^0$ and $Zh_1\varphi''^0$. Gauge boson decays can therefore not constrain the lower mass of $h_1$.
2) When $\varphi'^0$ or $\varphi''^0$ is the lightest state, we do not have an upper bound on this state by the heavy Higgs decays because the couplings $\varphi'^0W^+W^-$ ($\varphi''^0W^+W^-$) are absent. On the contrary we can have a lower bound by $W$ and $Z$ decay because couplings like $Z\varphi'^0\varphi''^0$ and $W^-\varphi'^0\varphi''^-$ are allowed.

### 5.9.2 The Alignment $(v, 0, 0)$

The second minimum we consider is $(v, 0, 0)$ that is $Z_2$ conserving. In this minimum, there is only one $Z_2$ even Higgs boson. We refer to this as $h_1$, although, again, it is not necessary the lightest one. There are also four $Z_2$ odd states: a degenerate pair of CP even bosons, labeled $h_{2,3}$ and a degenerate pair that is CP odd, labeled $h_{4,5}$. As in the previous subsection we sketch the expectations for a numerical analysis.

1) When $h_1$, the $Z_2$-even SM-like Higgs, is the lightest boson, we expect the SM Higgs upper bound to apply, but there should be no lower bound because the interactions $Zh_1h_{4,5}$ are forbidden by the $Z_2$ symmetry;
2) When the two lightest bosons are the $Z_2$ odd degenerate states $h_{2,3}$ (CP even) or $h_{4,5}$ (CP odd) we expect no upper bound. Moreover since they are degenerate we do not expect a lower bound either. On the contrary we expect that $Z$ and $W$ decays constrain the third lightest neutral Higgs mass and that of the charged ones.

In figure 5.3 we see a large number of points on the diagonal. This means that the lightest mass $m_1$ is identical to the second-lightest mass $m_2$, with values up to 700 GeV. Having one of the degenerate

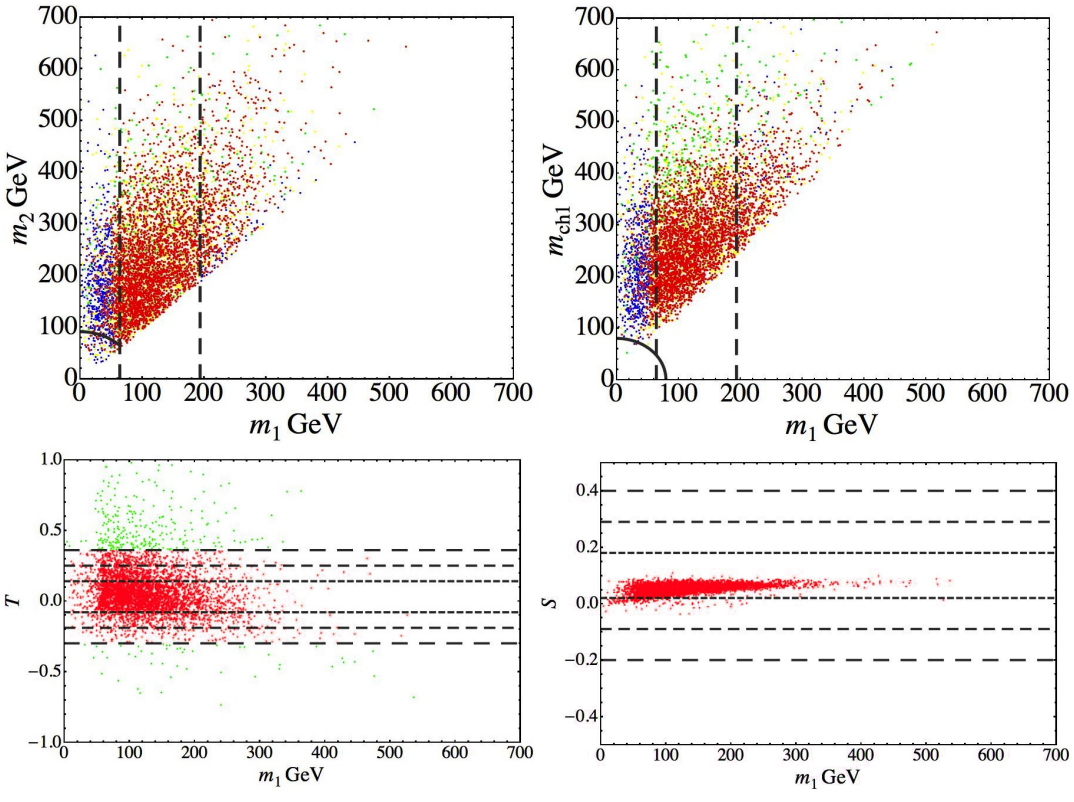


Figure 5.2: *The $Z_3$ conserving alignment $(v, v, v)$: the upper panels show the lightest neutral mass $m_1$ versus the second lightest neutral mass $m_2$ and versus the lightest charged one $m_{ch_1}$ respectively. The gray arc delimits the region below which the $Z$ $(W)$ decay channel opens. On the left plot the arc is only $45°$ because $m_2 \geq m_1$. For points below the arc the $Z$ $(W)$ decay can happen. The points allowed stretch in the region close to the border because of the conditions (5.69). The dashed vertical lines indicates the approximate cuts that occur at $m_1 \sim m_Z/\sqrt{2}$ and $m_1 \sim 194$ GeV according to case 2) and case 1) respectively as explained in the text. The lower panels show the contributions to $T$ and $S$ for the green and red points. The gray dashed lines indicate the experimental values at 3, 2, $1\sigma$ level with long, normal and short dashing respectively. $T$ turns out to be the most constraining oblique parameter.*

pairs as the lightest states reflects case 2). The points corresponding to case 1) have a sharp cut at $m_1 = 194$ GeV. This cut rejects many blue points, i.e. those that satisfy the unitarity constraint but not the decay constraint. We have also reported $m_1$ versus $m_3$ to check that indeed, when $m_1 \to 0$, $m_3$ is bounded by $m_Z$ as we expected. Our intuitions are also confirmed by the plot $m_1 - m_{ch_1}$, where $m_{ch_1}$ stands for the lightest charged Higgs. As in the $Z_3$ preserving case the most constraining oblique parameter is $T$.

### 5.9.3 The Alignment $(v_1, v_2, v_3)$ with $\epsilon = 0, \lambda_3 + \lambda_4 + \lambda_5 = 0$

In this case we do not have any surviving symmetry that forbids specific couplings as was the case in the previous two subsections. However from subsection 5.6.4 we know that the conditions $\epsilon = 0$, $\lambda_3 + \lambda_4 + \lambda_5 = 0$ give rise to two extra massless CP even particles. This justifies two expectations.

1) When the lightest massive state is CP odd, then its mass is bounded by the $Z$ decay through equation (5.69);

2) When the lightest massive state is CP even, then its mass could reach smaller values since the $Z$ decay bound would constrain the combination of its mass with the lightest CP odd state mass.

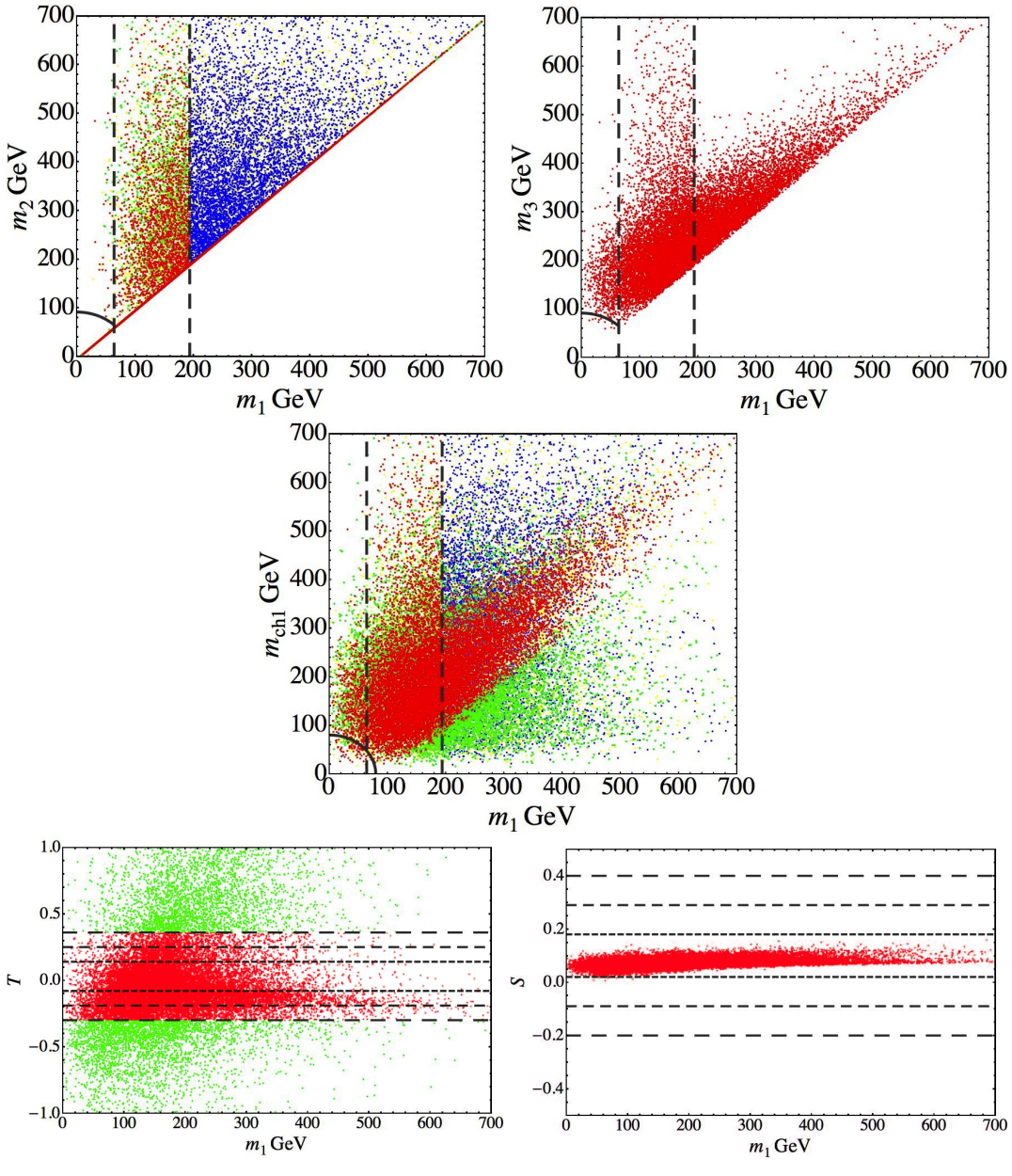


Figure 5.3: *The alignment* $(v, 0, 0)$*: the upper panels show* $m_1$ *versus* $m_2$ *(on the left) and third lightest* $m_3$ *(on the right). For the latter we reported only the R points. The central panel shows* $m_1$ *versus* $m_{ch_1}$*. The gray arc delimits the region below which the Z (W) decay channel opens while the second dashed vertical line indicates the SM-Higgs mass upper bound at* 194 *GeV. The first dashed vertical line at* $m_1 = m_Z/\sqrt{2}$ *is given to help a comparison with the* $Z_3$ *preserving case. On the first two plots the arc is only 45 degrees because* $m_{2,3} \geq m_1$*. The lower panels show the contributions to T and S. Again, the T parameter turns out to be the most constraining one.*

Moreover in both cases we expect the mass of the lightest charged scalar bounded by $W$ decay, according to equation (5.71), due to its coupling with $W$ and the massless particles.

Figure 5.4 shows that case 2) happens very rarely as there are very few red points below the $Z$ cut. As for the $Z_3$ and $Z_2$ preserving minima the $T$ parameter is the most constraining one. In general, we mention that it is remarkable that there are many red points in the figures. Even with extra massless particles present, it is quite possible to pass all electroweak tests.

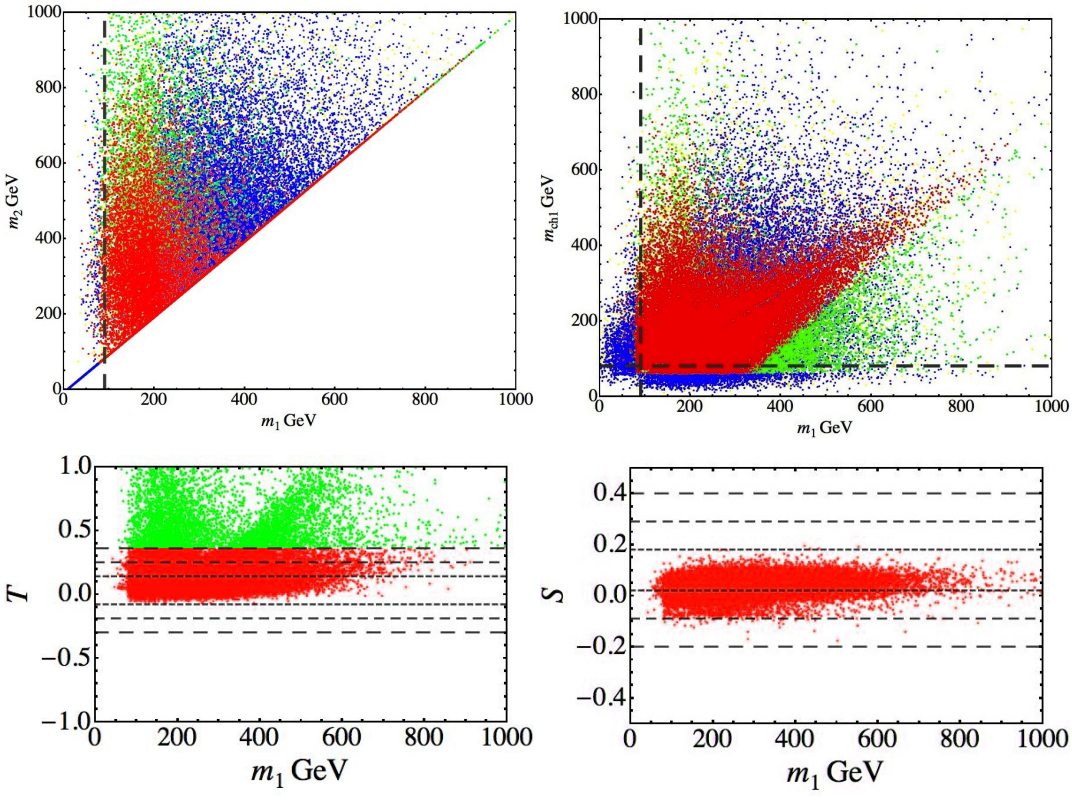


Figure 5.4: *The alignment $(v_1, v_2, v_3)$ with extra Goldstone bosons: the upper panels show $m_1$ versus $m_2$ and $m_{ch_1}$ respectively. The dashed lines at $m_1 = m_Z$ (vertical) and $m_{ch1} = m_W$ (horizontal) delimit the region below which the $Z$ and $W$ decay channels open respectively. The allowed points concentrate close to the borders according to equations 5.69-5.71. The lower panels show the contributions to $T$ and $S$. Again, the $T$ parameter turns out to be the most constraining one.*

### 5.9.4 The Alignment $(ve^{i\omega_1}, v, 0)$

The alignment $(ve^{i\omega_1}, v, 0)$ does not preserve any $A_4$ subgroup, just like the vacuum alignment $(v_1, v_2, v_3)$ discussed above. We expect that $Z$ decay does not give a lower bound on $m_1$ and $m_2$ in figure 5.5 as the two lightest Higgs might have the same CP eigenvalue, preventing the $Z$ to decay into them. $W$ decay on the other hand gives a lower bound on the quantity $m_1^2 + m_{ch_1}^2$. Regarding the upper bound on the lightest neutral mass state we do not expect any clear cut because we may not identify a SM-like Higgs.

### 5.9.5 The Alignment $(ve^{i\omega_1}, ve^{-i\omega_1}, rv)$ case $i)$

In section 5.6.8 we have seen that the alignment $(ve^{i\omega_1}, ve^{-i\omega_1}, rv)$ with the constrains $\lambda_5 = 0$, $\lambda_4 = -\lambda_3$, gives rise to 4 extra GBs and only to one neutral state. The expressions for the three non-vanishing masses (5.37) and (5.38) show that $\lambda_1$ and $\lambda_3$ should be positive in this case.

The positivity constraint is therefore easily met. Also the test of unitarity can be passed if the parameters are centred around 1. We expect that the most stringent bound is given by the decay constrains and not by the $T$, $S$ and $U$ parameters: massless particles give a small contribution to the oblique parameters and due to the limited number of new massive particles (two charged degenerate scalars) $T$, $S$ and $U$ should not deviate too much from the SM values. Indeed in figure 5.6 it is shown that the oblique parameters are not constraining at all at $3\sigma$ level. For this reason we only report the

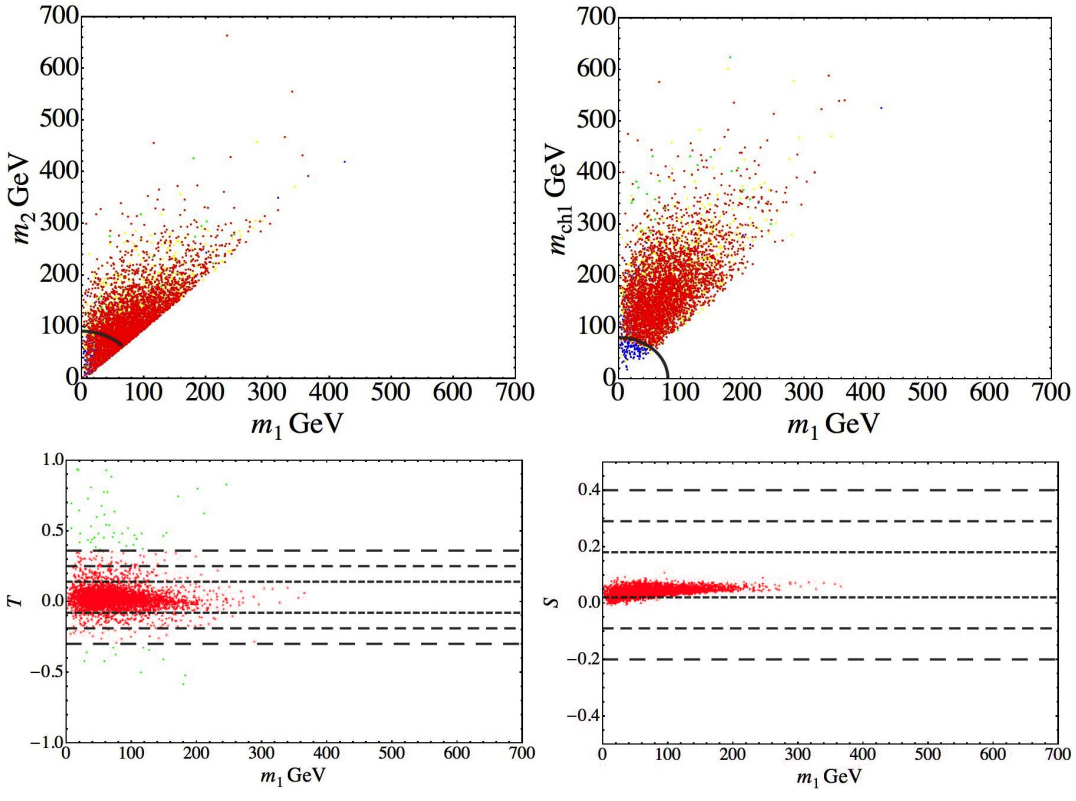


Figure 5.5: *The complex alignment* $(ve^{i\omega_1}, v, 0)$*: as in the previous figure the upper panels show* $m_1$ *versus* $m_2$ *and* $m_{ch_1}$ *respectively. In the plot on the right, the effect of the* $W$ *decay constraint on* $m_1^2 + m_{ch_1}^2$ *is clear by looking at the B points. The lower panels show the contributions to* $T$ *and* $S$*. Again, the* $T$ *parameter turns out to be the most constraining one.*

points R in the upper panel of figure 5.6. In the $m_1 - m_{ch_1}$ plot (obviously, the absence of a second neutral state prohibits a $(m_1 - m_2)$–plot), we see that with respect to the minima so far analyzed there are much fewer points and that as expected there are cuts in correspondence to $m_Z$ and $m_W$.

In conclusion, the solutions for the alignment $(ve^{i\omega_1}, ve^{-i\omega_1}, rv)$ with $\lambda_5 = 0$, $\lambda_4 = -\lambda_3$ are not easy to find, but the Higgs phenomenology does not completely rule out this vacuum configuration. We could introduce a weight to estimate the degree to which a solution is stable or fine-tuned, but this goes beyond the purposes of this work. We note however that this situation with four extra massless particles should be very problematic when considering the model dependent constraints. Indeed the two models with this vacuum studied in section 5.10 are of the second type, where there are no extra Goldstone bosons, although light states might be problematic.

### 5.9.6 $(ve^{i\omega_1}, ve^{-i\omega_1}, rv)$ case $ii)$

In section 5.6.8 we showed that at least in the three special limits $r \sim 0$, $r \sim 1$ and $r >> 1$, there are one or two very light particles.

It turns out that finding actual minima (i.e. solutions of equation (5.8) that are not saddle points) is very hard. Scanning over 100.000 points in parameter space with variable $r$, we only found a handful of minima (yellow or otherwise coloured points). This is sketched in figure 5.7. The other relevant information in this diagram is that for any value of $r$ the two lightest states are always very light, thus confirming our rough analytical approximations. Indeed both $m_1$ and $m_2$ are lighter then expected. This holds in particular for $m_2$ in case $r \sim 0$, where equation (5.41) just predicts one very light state. This indicates that some cancelations have to occur in order to make all masses greater than 0. This

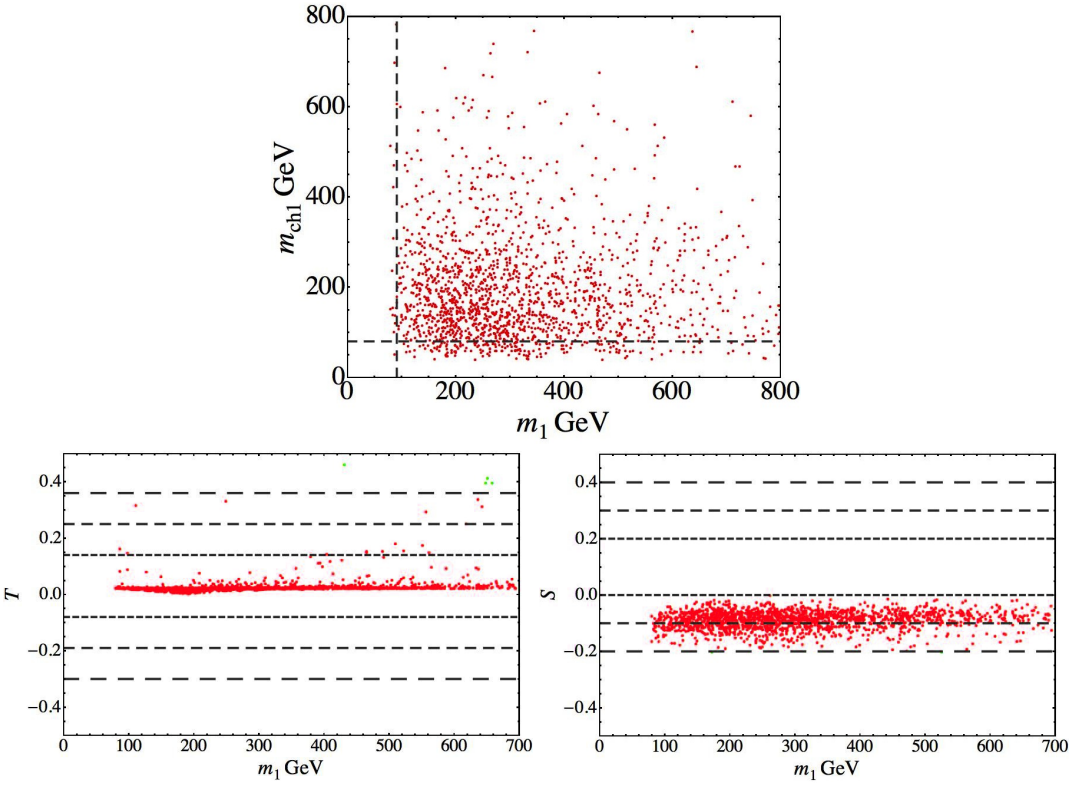


Figure 5.6: *Case $i$) of the alignment $(ve^{i\omega_1}, ve^{-i\omega_1}, rv)$ case $i$): the upper panel show $m_1$ versus $m_{ch_1}$. Only the R points are reported. The lower panels show the contributions to $T$ and $S$ for the G points. For this specific case the oblique parameter constraint is irrelevant compared to the decay one.*

might explain the difficulty to find solutions; this cannot to be ascribed to any constraint imposed, because even in presence of 4 additional Goldstone bosons as in section 5.9.5 there is a significant larger number of solutions.

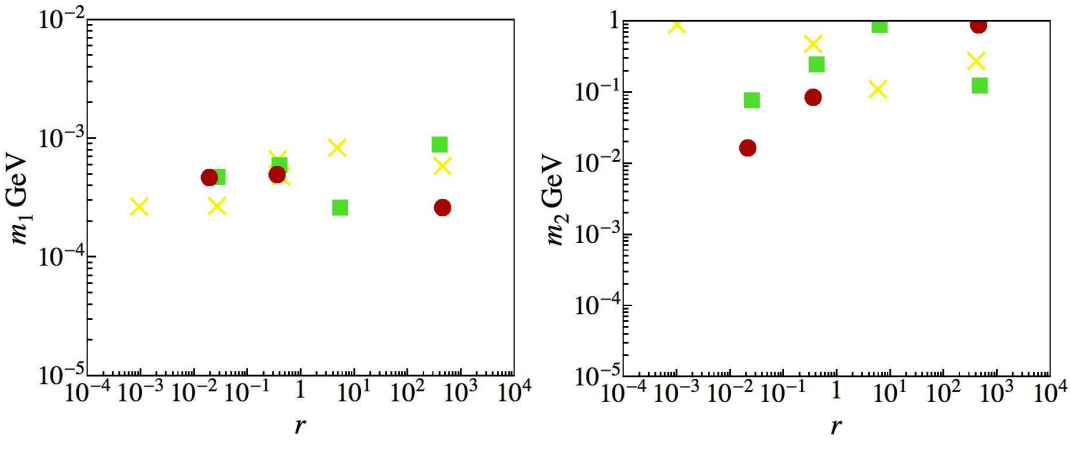


Figure 5.7: *Case $ii$) of the alignment $(ve^{i\omega_1}, ve^{-i\omega_1}, rv)$, the panels show $m_1$ (on the left) and $m_2$ (on the right) versus $r$. The number of points is small, but the most interesting information is the order of magnitude of the masses.*

It is possible to add soft $A_4$ breaking terms as given in equation (5.5) to the potential. All five neutral and all four charged Higgses can be in the LHC sensitive range between 100 GeV and 1 TeV if the

dimensionless parameters $m$, $n$, $k$ are approximately 0.05, corresponding to effective parameters of a few GeV after multiplying $n_{\text{soft,eff}} = \sqrt{m^2 + n^2 + k^2}$ by $v_{\text{ew}}$. It is interesting to underline that such large Higgs masses have been recovered by using soft terms at most of order of $5\%$ of the EW vev. This underlines a non-linear dependence, as can be seen in figure 5.8. In this figure $r$ is fixed to the large value of 240, in accordance with model 2 of the next section.

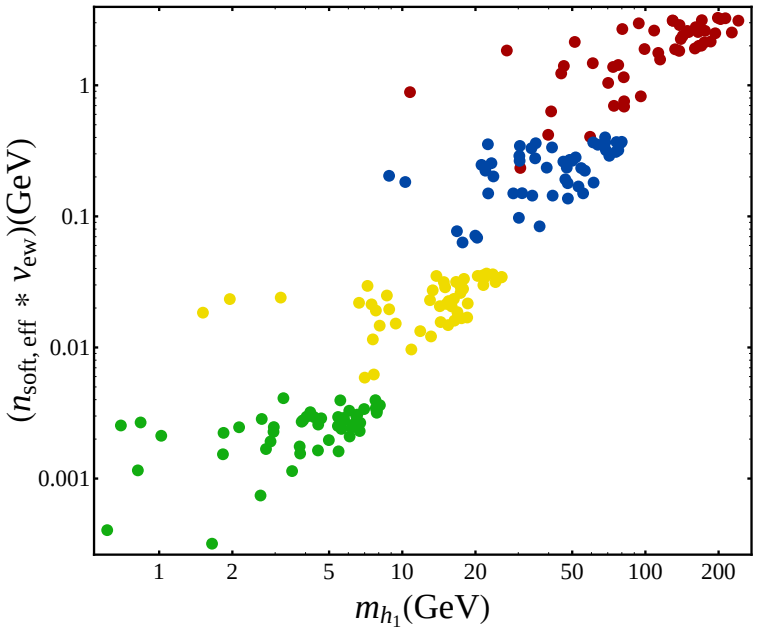


Figure 5.8: *Correlation among the lightest Higgs mass and the soft breaking parameter. The different colours correspond to the ranges that the individual parameters $m$, $n$ and $k$ are in, respectively $(0 - 10^{-4})$, $(0 - 10^{-3})$, $(0 - 10^{-2})$ and $(0 - 10^{-1})$*

## 5.10 Four models of flavour symmetries at the electroweak scale

In this section we describe four concrete models that contain a triplet of Higgses. In these models the $A_4$ representations of not only the Higgs sector are chosen, but also of the various Standard Model fermions. The model of Ma and Rajasekaran [97] (model 1) and the model of Morisi and Peinado [128] (model 2) focus on the lepton sector. The model of Lavoura and Kühböck [148] (model 3) describes the quark sector. In 'quark mixing in the discrete dark matter model' (model 4), we consider both sectors, but specifically focus on quarks.

Models 1 and 4 are non-minimal in the definition of section 5.3; models 2 and 3 are minimal. These two models use exactly the minimum we found to be the most problematic in the previous section. When analyzing the phenomenology in section 5.12 therefore, we allow for the presence of soft $A_4$ breaking terms.

### 5.10.1 Model 1

Model 1 [97] is an extension of a simpler model by one of the authors [149] that generates neutrino masses via a TeV-scale seesaw of type-I. In both models several Higgs fields occur, one of which carries lepton number. In [97] the choice is made to make the Higgs $SU(2)$-doublet that does not carry lepton number a triplet of $A_4$. The most general potential for this triplet of Higgses 5.4 is written down for the first time there. The triplet $\Phi_a$ couples only to charged leptons and the chosen

vacuum alignment falls in the class $(v, v, v)$, with $v$ real. In the original work, the constraint that the $\epsilon$ phase of the potential should be zero is assumed to make this alignment possible, but as shown in section 5.6.2 this is in fact not necessary.

All the time there is also a fourth Higgs doublet. This is a singlet $\eta$ of $A_4$ and, as mentioned above, it carries a single unit of lepton number. The appearance of a singlet next to the triplet makes this model clearly a non-minimal one. Two new terms are added to the scalar potential (5.4)

$$\begin{aligned} V_\eta &= \mu_\eta^2(\eta^\dagger\eta) + \lambda_\eta(\eta^\dagger\eta)^2 + \lambda_{\eta\Phi}(\eta^\dagger\eta)(\phi_1^\dagger\phi_1 + \phi_2^\dagger\phi_2 + \phi_3^\dagger\phi_3) \\ V_{\eta\,soft} &= \mu_{\eta\Phi}^2\left[\eta^\dagger(\phi_1+\phi_2+\phi_3) + (\phi_1^\dagger+\phi_2^\dagger+\phi_3^\dagger)\eta\right], \end{aligned} \tag{5.79}$$

where the $A_4$ soft breaking part $V_{\eta\,soft}$ is needed in order to avoid additional GBs. $V_{\eta\,soft}$ breaks $A_4$ as well as lepton number, but preserves its $Z_3$ subgroup thus the full potential may naturally realize the vacuum configuration

$$\langle\Phi\rangle \sim (v, v, v), \qquad \langle\eta\rangle \sim v_\eta \propto \mu_{\eta\Phi}^2 v. \tag{5.80}$$

The vacuum expectation value of the field $\eta$ is much smaller than that of $\Phi$. This relates to the relative smallness of $\mu_{\eta\Phi}^2$ that is natural in the sense that if it goes to zero the model's symmetry is increased because lepton number is unbroken. This makes $v_\eta$ very fit to generate the (small) neutrino masses.

The fermion content of the model is much like the (later constructed) Altarelli–Feruglio model of section 2.4: the lepton doublet is a triplet of $A_4$ and the righthanded charged fermions are singlets of respectively type 1, $1'$ and $1''$. A righthanded neutrino is present as $A_4$-triplet – which is indeed also Altarelli and Feruglio's choice in the seesaw version of their model. It is interesting to note that this righthanded neutrino has zero lepton number. The complete fermion and Higgs content of the model is given in table 5.1.

| Field | $L_L$ | $e_R$ | $\mu_R$ | $\tau_R$ | $\nu_R$ | $\Phi$ | $\eta$ |
|---|---|---|---|---|---|---|---|
| $A_4$ | 3 | 1 | $1'$ | $1''$ | 3 | 3 | 1 |
| lepton number | 1 | 1 | 1 | 1 | 0 | 0 | -1 |

Table 5.1: The lepton and Higgs content of model 1.

Lepton number constrains the triplet $\Phi$ to couple only to charged leptons and the singlet $\eta$ to participate only in the neutrino Dirac terms:

$$\mathcal{L} = \frac{1}{2}M\nu_{Ri}^2 + f\bar{\nu}_{Ri}L_{Li}\eta + Y_{ijk}\bar{L}_{Li}l_{Rj}\Phi_k + \text{h.c.} \tag{5.81}$$

In this formula, $l_R$ is general notation for the three righthanded charged leptons. The Yukawa matrices in the charged lepton sector are

$$Y_{ij1} = \begin{pmatrix} y_1 & y_2 & y_3 \\ 0 & 0 & 0 \\ 0 & 0 & 0 \end{pmatrix}, \quad Y_{ij2} = \begin{pmatrix} 0 & 0 & 0 \\ y_1 & \omega y_2 & \omega^2 y_3 \\ 0 & 0 & 0 \end{pmatrix}, \quad Y_{ij3} = \begin{pmatrix} 0 & 0 & 0 \\ 0 & 0 & 0 \\ y_1 & \omega^2 y_2 & \omega y_3 \end{pmatrix} \tag{5.82}$$

After the diagonalization of the charged lepton mass matrix, it is straightforward to relate the coefficient $y_i$ to the mass eigenvalues:

$$y_1 = \frac{m_e}{\sqrt{3}v}, \quad y_2 = \frac{m_\mu}{\sqrt{3}v}, \quad y_3 = \frac{m_\tau}{\sqrt{3}v}. \tag{5.83}$$

Since the vevs of the scalar potential are real, the $U$ matrix that rotates the Higgs fields into the mass basis (2.54) is block diagonal. Neutrino masses are given through the type I See-Saw and have magnitude $f^2u^2/M$. Due to the smallness of $v_\eta$, the righthanded neutrino masses can be at a (relatively) low scale around a TeV. Maximal mixing in the $(\mu\ \tau)$ sector is obtained and depending on soft $A_4$ breaking terms for the righthanded neutrinos, specific mixing patterns like the bimaximal or the tribimaximal are possible.

### 5.10.2 Model 2

The second model we discuss is the one by Morisi and Peinado [128]. Like model 1, this model focuses on the lepton sector, but four important choices are different with respect to the work of Ma and Rajasekaran. The first is that this model does not employ an $A_4$-singlet Higgs; all the Higgs fields present are in the triplet $\Phi$.

The second difference is in the vacuum of the $\Phi$ field. This is a permutation of the complex vacuum introduced in section 5.6.8 – in particular of case $ii)$ of that section, as the potential parameters are not constrained.

$$\langle \Phi \rangle = \frac{v_{ew}}{\sqrt{2+r^2}} \left( r, \quad e^{i\omega_1}, \quad e^{-i\omega_1} \right) . \tag{5.84}$$

As shown below, $r$ needs to be very large in order to incorporate the charged lepton masses: $r \simeq 240$. This case was studied in detail in sections 5.6.8 and 5.9.6, where it was concluded that in order for this minimum to be viable, the potential needs a contribution from soft breaking terms. When we study the fermion-dependent processes in section 5.12, we indeed assume these terms to be present.

Thirdly, models 1 and 2 differ in the choice of fermion representations. In model 2, the choice is made to put all relevant fields in the triplet representation of $A_4$. Table 5.2 that shows the content of the model is therefore very simple

| Field | $L_L$ | $l_R$ | $\Phi$ |
|---|---|---|---|
| $A_4$ | 3 | 3 | 3 |

Table 5.2: The lepton and Higgs content of model 2.

The Yukawa Lagrangian for the charged leptons is also very simple. It contains the two possible ways to contract three $A_4$ triplets to a singlet.

$$\mathcal{L} = y_1 \Big( \bar{L}_{L1} \Phi_3 l_{R2} + \bar{L}_{L2} \Phi_1 l_{R3} + \bar{L}_{L3} \Phi_2 l_{R1} \Big) + y_2 \Big( \bar{L}_{L1} \Phi_2 l_{R3} + \bar{L}_{L2} \Phi_3 l_{R1} + \bar{L}_{L3} \Phi_1 l_{R2} \Big) . \tag{5.85}$$

When the three Higgs fields obtain their vevs as in equation 5.84, this results in a charged lepton mass matrix without diagonal components:

$$M_l = \begin{pmatrix} 0 & a & b \\ b & 0 & ar \\ a & br & 0 \end{pmatrix} . \tag{5.86}$$

Here $a = y_1 v_{ew}/\sqrt{2+r^2} = 0.43$ MeV; $b = y_2 v_{ew}/\sqrt{2+r^2} = 7.3$ MeV and, as mentioned before, $r = 242$. The mass matrix is real because all phases can be absorbed in the fields.

The fourth and last important difference between model 1 and 2 is that in the latter neutrino masses originate from effective dimension-5 operators. To a good approximation the neutrino mass matrix is

$$M_\nu = \begin{pmatrix} x r^2 & \kappa r e^{-i\omega_1} & \kappa r e^{i\omega_1} \\ \kappa r e^{-i\omega_1} & z r^2 & \kappa \\ \kappa r e^{i\omega_1} & \kappa & y r^2 \end{pmatrix} . \tag{5.87}$$

In this matrix $x$, $y$, $z$ and $\kappa$ are linear combinations of the parameters that occur in the effective Lagrangian. In the limit where $\omega_1 \to 0$ and $y \to z$, the neutrino mass matrix is $(\mu\ \tau)$-invariant, implying maximal atmospheric and zero reactor mixing angle. The solar mixing angle, however, is undetermined.

### 5.10.3 Model 3

In model 3, constructed by Lavoura and Kühböck [127], the quark sector is central. The minimum configuration of the Higgs fields is, up to permutations, the same as in model 2 (with model 3 having the priority), although the value of $r$ used is smaller, $r \simeq 43$, bringing the model less deep into the $r \gg 1$ limit. The presence of soft $A_4$-breaking terms is thus also mandatory for this model. Figure 5.8 that shows the behaviour of the lightest Higgs as a function of the soft breaking terms, was constructed for the parameters of model 2; for those of model 3, it looks very similar.

The fermion representation chosen are the triplet for the lefthanded doublets and three different singlets $1$, $1'$ and $1''$ for both types of righthanded quarks; see also table 5.3.

| Field | $Q_L$ | $u_R$ | $c_R$ | $t_R$ | $d_R$ | $s_R$ | $b_R$ | $\Phi$ |
|---|---|---|---|---|---|---|---|---|
| $A_4$ | 3 | 1 | $1'$ | $1''$ | 1 | $1'$ | $1''$ | 3 |

Table 5.3: The lepton and Higgs content of model 3.

This fermion assignment is much like that of model 1, with quarks replacing charged leptons and indeed the Yukawa Lagrangian and matrices have the same structure. The relevant Lagrangian reads

$$\mathcal{L} = Y^d_{ijk}\bar{Q}_{Li}d_{Rj}\Phi_k + Y^u_{ijk}\bar{Q}_{Li}u_{Rj}\tilde{\Phi}_k + \text{h.c.} \tag{5.88}$$

Here $\tilde{\Phi} = i\sigma_2\Phi^*$ to provide up-type Higgs bosons. This Lagrangian corresponds to the mass matrices for the down quarks (cf. equation (5.82))

$$M^d = \begin{pmatrix} y_1 & y_2 & y_3 \\ 0 & 0 & 0 \\ 0 & 0 & 0 \end{pmatrix} \frac{v_{ew}}{\sqrt{2+r^2}} e^{i\omega_1} + \begin{pmatrix} 0 & 0 & 0 \\ y_1 & \omega y_2 & \omega^2 y_3 \\ 0 & 0 & 0 \end{pmatrix} \frac{v_{ew}}{\sqrt{2+r^2}} e^{-i\omega_1} + \begin{pmatrix} 0 & 0 & 0 \\ 0 & 0 & 0 \\ y_1 & \omega^2 y_2 & \omega y_3 \end{pmatrix} \frac{r v_{ew}}{\sqrt{2+r^2}} . \tag{5.89}$$

The up Yukawa matrices have the same structure, but with $y_4$, $y_5$ and $y_6$ as parameters and the phases reversed (due to the complex conjugation in equation (5.88). The eight parameters of the model $y_1 - y_6$, $r$ and $\omega_1$ can now be fit against nine observables in the quark sector (the six quark masses and the three CKM angles). This fit has a minimum corresponding to $\chi^2 = 0.057$ and parameters given by

$$\begin{array}{rclrclrcl} y_1 &=& 0.010, & y_2 &=& 0.022, & y_3 &=& 0.00058, \\ y_4 &=& 0.97, & y_5 &=& 0.127, & y_6 &=& 0.00026, \\ r &=& 43, & \omega_1 &=& 0.23 \text{ rad.} & & & \end{array} \tag{5.90}$$

All three angles of the CKM matrix are fit very well by the parameters given above, but the phase is not. The CKM matrix that is the result of the construction of model 3 is completely real, providing no source of CP violation.

### 5.10.4 Model 4 - Quark mixing in the discrete dark matter model

In model 4 we present an extension of a number of studies [150–152] in which the concept of discrete dark matter (DDM) is developed. In these works, the focus is on the scalar sector, but also charged leptons are discussed, although quarks are not. In our work, we add quarks to the set up and allow for quark mixing in a way that is much like the one described in chapter 4.

At a number of places in this thesis we have seen the connection between symmetries and the presence of a dark matter candidate in a theory. Examples were the axion of section 1.3.1 and the 'lightest supersymmetric particle' (LSP) of section 1.3.2. The key to the relation between symmetry and dark matter is that a symmetry can prevent the decay of a particle, thus making it stable and letting it exist in the cosmos. It is a very natural question to ask whether flavour symmetries can

provide a dark matter candidate. Note that this question is less relevant in models where flavour symmetries are combined with supersymmetry or extra dimensions, as those on themselves already provide a dark matter candidate. In the models of this section on the other hand, where flavour symmetry is the only relevant symmetry beyond the Standard Model, the question becomes more interesting.

The naive answer to the question of the previous paragraph is 'no'. Flavour symmetries cannot provide a dark matter candidate, because flavour symmetries are always broken when flavons (or Higgs fields in non-trivial representations of the flavour group) develop vacuum expectation values. In some cases, however, there is a residual symmetry after a flavour symmetry is broken. In this chapter we have seen that there is a residual symmetry $Z_3$ when the three Higgses have their vevs as $(v, v, v)$ and $Z_2$ when the vev alignment is $(v, 0, 0)$. Those residual symmetries can well be the symmetries that make a dark matter candidate stable.

In [150] the vacuum $(v, 0, 0)$ is selected, while also a $A_4$-singlet Higgs is present. The inert fields $\Phi_2$ and $\Phi_3$ give rise to four neutral Higgs bosons: two scalars $h_2$ and $h_3$ and two pseudo scalars $A_2$ and $A_3$. The lightest of these cannot decay and is a dark matter candidate. Note that even if the dark matter candidate cannot decay, a pair of two candidates can annihilate. In [152] it is shown that the correct relic abundance can still be obtained for a dark matter mass $M_{DM}$ in the large range 1 - 100 GeV. In our set up, additional annihilation channels to quarks are added and the relic density is a crucial test of the viability of the extension as discussed in section 5.12.

The matter content of the model is given in table 5.4. We see that in this model all charged fermion fields, both left- and righthanded are in the various singlet representations of $A_4$. Note that all these $A_4$ singlets transform under the $Z_3$ subgroup of $A_4$, but not under the $Z_2$ subgroup, making them even under the residual symmetry. There are four righthanded neutrinos originating from a $A_4$ triplet and a singlet. The second and third component of the neutrino triplet are odd under the residual $Z_2$ just like the corresponding components of the Higgs triplet.

| Field | $\Phi$ | $\eta$ | $Q_{L_1}$ | $Q_{L_2}$ | $Q_{L_3}$ | $q_{R_1}$ | $q_{R_2}$ | $q_{R_3}$ |
|---|---|---|---|---|---|---|---|---|
| $A_4$ | 3 | 1 | 1 | $1'$ | $1''$ | 1 | $1'$ | $1''$ |
| Field | $L_{L_e}$ | $L_{L_\mu}$ | $L_{L_\tau}$ | $l_{R_e}$ | $l_{R_\mu}$ | $l_{R_\tau}$ | $\nu_{R_T}$ | $\nu_{R_4}$ |
| $A_4$ | 1 | $1'$ | $1''$ | 1 | $1'$ | $1''$ | 3 | 1 |

Table 5.4: *The $A_4$ representations of the fields in model 4; $q = u, d$.*

The resulting Yukawa Lagrangian for the quarks reads

$$\begin{aligned}\mathcal{L}_{\rm q} = &y_u\overline{Q}_1\tilde{\eta}u_{1R} + y_c\overline{Q}_2\tilde{\eta}u_{2R} + y_t\overline{Q}_3\tilde{\eta}u_{3R}+\\ &y_d\overline{Q}_1\eta d_{1R} + y_s\overline{Q}_2\eta d_{2R} + y_b\overline{Q}_3\eta d_{3R} + \text{h.c.},\end{aligned} \tag{5.91}$$

Here the up-type Higgs $\tilde{\eta}$ is defined analogously to $\tilde{\Phi}$ as given below equation (5.88).

At the renormalisable level, both up- and down-quark matrices are diagonal with all masses given by $m_i = y_i v_\eta/\sqrt{2}$, with $v_\eta/\sqrt{2}$ the vacuum expectation value of the $A_4$-singlet Higgs field. Obviously, at this level, the CKM matrix is the identity matrix.

For the leptons, the Lagrangian is the same as in [150]

$$\begin{aligned}\mathcal{L}_{\rm l} = &y_e\overline{L}_e l_{Re}\eta + y_\mu\overline{L}_\mu l^c_{R\mu}\eta + y_\tau\overline{L}_\tau l^c_{R\tau}\eta+\\ &y_1^\nu\overline{L}_e(\nu_{R_T}\tilde{\Phi})_1 + y_2^\nu\overline{L}_\mu(\nu_{R_T}\tilde{\Phi})_{1'} + y_3^\nu\overline{L}_\tau(\nu_{R_T}\tilde{\Phi})_{1''}+\\ &y_4^\nu\overline{L}_e\nu_{R_4}\eta + M_1N_TN_T + M_2N_4N_4 + \text{h.c.}\end{aligned} \tag{5.92}$$

This leads to charged lepton masses similar to the quark masses and a light neutrino mass matrix of

the form

$$M_\nu = \frac{v_\Phi^2}{2M_1}\begin{pmatrix} (y_1^\nu)^2 + (y_4^\nu)^2\frac{M_1}{M_2}\frac{v_\eta}{v_\Phi} & y_1^\nu\, y_2^\nu & y_1^\nu\, y_3^\nu \\ y_1^\nu\, y_2^\nu & (y_2^\nu)^2 & y_2^\nu\, y_3^\nu \\ y_1^\nu\, y_3^\nu & y_2^\nu\, y_3^\nu & (y_3^\nu)^2 \end{pmatrix} . \tag{5.93}$$

The neutrino mass matrix has one zero eigenvalue, so a prediction of the model is one massless neutrino. The (1 3) mixing angle is zero at the renormalizable level. The other two angles are not determined and a simple tuning can reproduce the tribimaximal mixing pattern.

Quark mixing (and additional lepton mixing) can be generated by dimension six operators that contain extra insertions of the Higgs fields. There are three ways to contract the $SU(2)$ indices, represented by brackets in the equation below

$$\frac{f_{ij}}{\Lambda^2}(\overline{Q}_i\hat{H})d_j(\eta^\dagger\eta) + \frac{f'_{ij}}{\Lambda^2}(\overline{Q}_i\eta)d_j(\eta^\dagger\hat{H}) + \frac{f''_{ij}}{\Lambda^2}(\overline{Q}_i\eta)d_j(\hat{H}^\dagger\eta)\,. \tag{5.94}$$

The contraction of $A_4$ indices between the two $\eta^{(\dagger)}$ triplets is such that it generates the right type of singlet (1, 1′ or 1″) to match the charges for $\overline{Q}_i$ and $d_j$. It is important to note that this is possible for any combination of $i$ and $j$ due to the product rules of $A_4$, giving non-zero entries at all elements of the mass matrix. $\Lambda$ is the cut-off scale, up to which we accept the theory to be valid and the $f$ couplings are dimensionless. Analogous dimension-6 operators can obviously be constructed for up-type quarks and charged leptons.

The mass term Lagrangian (5.91) and the effective couplings (5.94) generate the effective mass matrix for down-type quarks

$$M_d = \begin{pmatrix} m_d & 0 & 0 \\ 0 & m_s & 0 \\ 0 & 0 & m_b \end{pmatrix} + \frac{v_H v_\eta^2}{\Lambda^2}\begin{pmatrix} h_{dd} & h_{ds} & h_{db} \\ h_{sd} & h_{ss} & h_{sb} \\ h_{bd} & h_{bs} & h_{bb} \end{pmatrix} + \mathcal{O}(\frac{1}{\Lambda^4})\,, \tag{5.95}$$

where $h_{ij} = (f_{ij} + f'_{ij} + f''_{ij})/2\sqrt{2}$. Analogous expressions again hold for up-type quarks and charged leptons.

The crucial question is how large the cut-off scale $\Lambda$ is. In principle, this is a scale we are free to set. Only using 'naturalness' and 'finetuning' arguments, we can find a range for it. We give two arguments, both pointing to a scale of 1 to 10 TeV.

In the first argument, we demand that there should not be more than 10 to 100% corrections to the Higgs from one-loop corrections to the Higgs propagator with the fermions and the (new) scalars of the theory. These corrections are typically of the order $\Lambda^2/(4\pi)^2$ and requiring them to be not too large with respect to $v_{ew}^2 = (246\text{GeV})^2$ indeed gives $\Lambda \lesssim (1 \text{ to } 10)$ TeV.

Interestingly, we find the same scale from an argument where we require the dimensionless parameters $h$, in particular $h_{ds}$, to be of order 1. The off-diagonal terms in equation (5.95) are responsible for generating the quark mixing as parameterized by the CKM matrix. As we do not have information about the size of the dimensionless parameters $h$, we assume them to be of order 1, which can be seen as the most natural assumption for dimensionless parameters.

Under this assumption, the absolute values of the corrections to the leading order elements of the mass matrix are of the same order for the up-type quark matrix and the down-type quark matrix. However, due to the much larger elements of the leading order up-type quark mass matrix, the effects on quark mixing are dominated by the down-type quark contributions. This allows us to estimate the order of magnitude of the cut-off scale.

Now the (1 2) element of equation (5.95) should be of order $\lambda_C\, m_s$ in order to reproduce the Cabibbo angle.

$$h_{ds}\frac{v_H v_\eta^2}{\Lambda^2} = \lambda_C m_s. \tag{5.96}$$

We define a parameter $\tan\tilde{\beta}$ as the ratio between the vev of $\eta$ and $\Phi$ in the same spirit as in 'normal' models where two Higgs doublet acquire a vev. With this definition, we can solve the previous equation for $\Lambda^2$

$$\Lambda^2 = h_{ds}\frac{v_H v_\eta^2}{\lambda_C m_s} = h_{bd}\frac{v_{ew}^3}{(\tan^2\tilde{\beta})(1+\frac{1}{\tan^2\tilde{\beta}})^{3/2}\lambda_C m_s} = [(1 \text{ to } 10)\text{ TeV}]^2. \tag{5.97}$$

The exact value depends on the exact values of $h_{ds}$ and $\tan\tilde{\beta}$; to obtain the range, we have taken them between 0.1 and 1 and between 0.1 and 10 respectively. The mass of the bottom quark is rather large and therefore the effect of $h_{db}$ and $h_{sb}$ $\theta_{13}$ and $\theta_{23}$ is relatively minor even if these parameters are of the same size as $h_{ds}$. This naturally keeps these angles smaller than the Cabibbo angle. Indeed in a large part of parameter space, we can fit them to their measured values.

The analogue of the dimension 6 operator (5.94) affects the lepton mixing. The fact that the down-type quark and charged lepton mass matrices are alike (at least at leading order) suggests that the matrices that diagonalize them, $V_L^d$ and $V_L^e$ are also similar. We thus expect a large angle (of the order of the Cabibbo angle) in the (1 2) sector of $V_L^e$. In the lepton mixing matrix $V_{\rm PMNS} = (V_L^e)^\dagger V_L^\nu$, this affects all three angles. In particular, we predict a Cabibbo-sized correction to the $\theta_{13}$-angle, bringing it in the range of the current fits given in table 2.4.

The cut-off scale $\Lambda$ may coincide with the scale $M_1$ that appears in the neutrino mass matrix (5.93). In that case, the seesaw mechanism indeed takes place at a low energy scale, 1 TeV, as compared to $10^{12}$ GeV as in chapter 4. In this case, the parameters $y_i^\nu$ should not be too small, $y_\nu = 10^{-(4\div 5)}$.

## 5.11 Description of model dependent tests of flavour symmetries at the electroweak scale

The interaction of fermions with the Higgs particles induces flavour violating processes in the lepton and quark sectors. In the first one, rare decays of muon and tau particles into three leptons are allowed at tree-level, while processes as $l_i \to l_j\gamma$ take place through one-loop graphs. For the quarks the possibility of $\Delta F = 2$ meson-antimeson oscillations is considered.

In this section we study these processes and obtain formulas that give the contribution of the new physics processes. We rely heavily on the equations obtained in section 2.2.5 where we have described the interactions of different fermions with multiple Higgs bosons. The formulas derived in this section are used in the next one, where we discuss to what degree they constrain the four models of the previous section.

### 5.11.1 The Processes $\mu^- \to e^-e^-e^+$ and $\tau^- \to \mu^-\mu^-e^+$

We consider the decay of a muon into a positron and two electrons as given in figure 5.9 on the left. In the approximation of massless final states, the decay amplitude is written as

$$\Gamma(\mu \to ee\overline{e}) = \frac{m_\mu^5}{(4\pi)^3\times 24} I_{\mu eee}\,. \tag{5.98}$$

The coefficient $I_{\mu eee}$ is a combination of $I_{ij}$ and $J_{ij}$, that were defined in section 2.2.5.

$$I_{\mu eee} = \left|\sum_\alpha \frac{I_{\mu e}^\alpha I_{ee}^\alpha}{m_H^{\alpha\,2}}\right|^2 + \left|\sum_\alpha \frac{J_{\mu e}^\alpha J_{ee}^\alpha}{m_H^{\alpha\,2}}\right|^2 + \left|\sum_\alpha \frac{I_{\mu e}^\alpha J_{ee}^\alpha}{m_H^{\alpha\,2}}\right|^2 + \left|\sum_\alpha \frac{J_{\mu e}^\alpha I_{ee}^\alpha}{m_H^{\alpha\,2}}\right|^2. \tag{5.99}$$

The prediction for the corresponding branching ratio is

$$\text{Br}(\mu \to ee\overline{e}) \approx \frac{\Gamma(\mu \to ee\overline{e})}{\Gamma(\mu \to e\overline{\nu}_e\nu_\mu)} = \frac{I_{\mu eee}}{8G_F^2}\,. \tag{5.100}$$

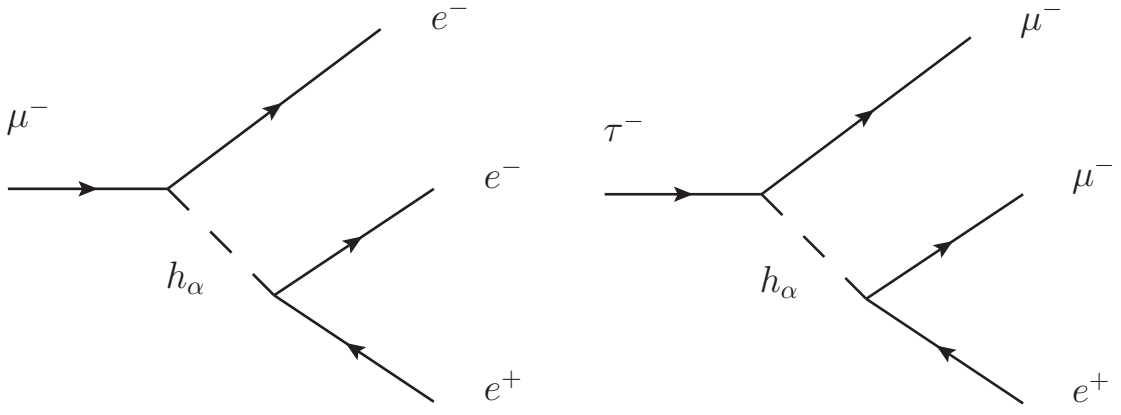


Figure 5.9: *The decays $\mu^- \to e^+e^-e^-$ (left) and $\tau^- \to e^+\mu^-\mu^-$ (right) can occur at tree level in our models.*

This is to be compared with the experimental limit [6] of $\text{Br}(\mu \to ee\overline{e})_{exp} \leq 1.0 \times 10^{-12}$.

The decay of a $\tau$ into two muons and a positron (figure 5.9 on the right) is generally less constrained that the decay of the muon in two electrons and a positron, but it is of interest in models where the latter process is prohibited by the symmetries. The calculation proceeds in an analogous way. The decay amplitude is now

$$\Gamma(\tau \to \overline{e}\mu\mu) = \frac{m_\tau^5}{(4\pi)^3 \times 24} I_{\tau\mu\mu e} \ . \tag{5.101}$$

The coefficient $I_{\tau\mu\mu e}$ is now given by the following expression:

$$I_{\tau\mu\mu e} = \left| \sum_\alpha \frac{I^\alpha_{\tau\mu} I^\alpha_{e\mu}}{{m^\alpha_H}^2} \right|^2 + \left| \sum_\alpha \frac{J^\alpha_{\tau\mu} J^\alpha_{e\mu}}{{m^\alpha_H}^2} \right|^2 + \left| \sum_\alpha \frac{I^\alpha_{\tau\mu} J^\alpha_{e\mu}}{{m^\alpha_H}^2} \right|^2 + \left| \sum_\alpha \frac{J^\alpha_{\tau\mu} I^\alpha_{e\mu}}{{m^\alpha_H}^2} \right|^2 . \tag{5.102}$$

The branching ratio becomes

$$\text{Br}(\tau \to \overline{e}\mu\mu) = 0.17 \times \frac{\Gamma(\tau \to \overline{e}\mu\mu)}{\Gamma(\tau \to \mu\overline{\nu}_\mu\nu_\tau)} = 0.17 \times \frac{I_{\tau\mu\mu e}}{8G_F^2}, \tag{5.103}$$

This branching ratio should be compared with the experimental limit [6] $\text{Br}(\tau \to \overline{e}\mu\mu)_{exp} \leq 2.3 \times 10^{-8}$ .

### 5.11.2 The process $\mu^- \to e^-\gamma$

The relevant diagram for the decay of the muon to an electron and a photon has one loop with a charged fermion and a neutral Higgs (see figure 5.10). We consider the limit in which the Higgs is much heavier than the virtual fermion and the final electron is massless. Under this assumption the decay amplitude becomes [153]

$$\Gamma(\mu \to e\gamma) = \frac{e^2 m_\mu^5}{6 \times (16)^3 \pi^5} \left| \sum_{\alpha,f} \frac{(R^\alpha_{fe})^* R^\alpha_{f\mu}}{{m^\alpha_H}^2} \right|^2 \tag{5.104}$$

This uses the coupling tensor $R$ defined in section 2.2.5. The branching ratio is

$$\text{Br}(\mu \to e\gamma) = \frac{\Gamma(\mu \to e\gamma)}{\Gamma(\mu \to e\nu\overline{\nu})} = \frac{\alpha_{em}}{32\pi G_F^2} \left| \sum_{\alpha,f} \frac{(R^\alpha_{fe})^* R^\alpha_{f\mu}}{{m^\alpha_H}^2} \right|^2 \tag{5.105}$$

This should be compared with the current experimental bound from MEGA [154] of $10^{-11}$ and the future experimental bound from MEG [155] of $(10^{-13})$.

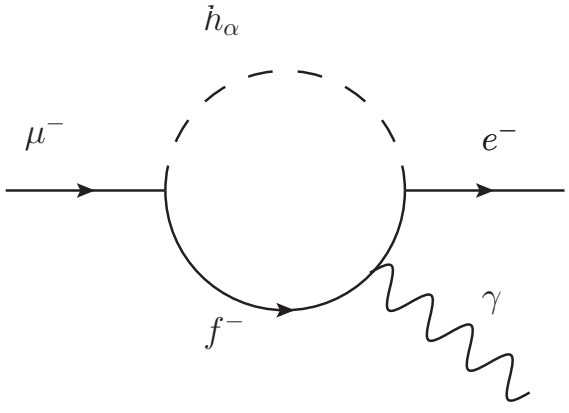


Figure 5.10: *The decays $\mu^- \to e^-\gamma$ proceeds at one loop in our models, but can be much larger than in the Standard Model, where a GIM-like cancellation occurs.*

### 5.11.3 Meson oscillations

Meson-antimeson oscillations are constrained to be generated by box processes in the SM (figure 5.11 on the left), but in the presence of flavour violating Higgs couplings, they can also proceed via tree-level Higgs exchange. Note that there is a large difference with the lepton processes. Those practically have zero background from the Standard Model and experimentally there are only upper bounds. Meson oscillations have been measured and fit fairly well to the Standard Model calculations. It is preferred that the new physics contributions are much smaller than the Standard Model, although in principle they can be of comparable magnitude if there is cancellation at the amplitude level.

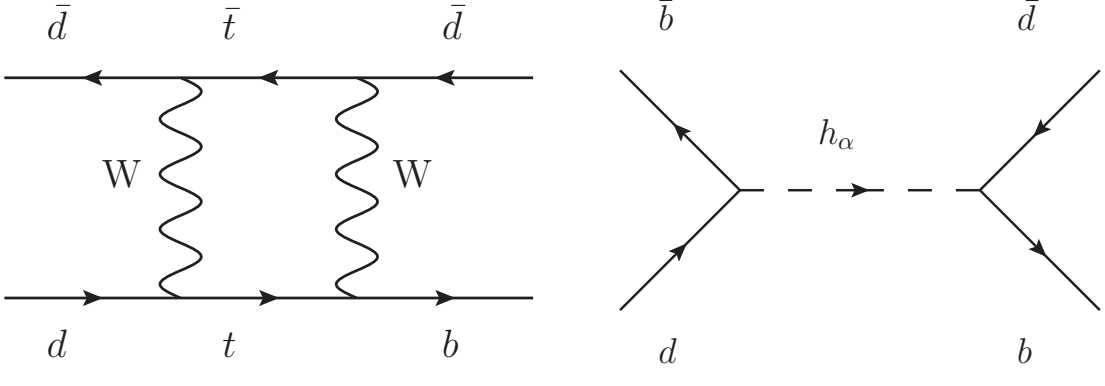


Figure 5.11: *$B_d$-$\overline{B}_d$ oscillations take place via box diagrams in the Standard Model, but can proceed via tree-level Higgs exchange in multi-Higgs models.*

For the mass splitting connected to $F^0 - \overline{F}^0$ oscillations [156, 157], we find

$$\Delta M_F = B_F^2\, f_F^2\, M_F \sum_\alpha \left[\frac{1}{{m_H^\alpha}^2}\Big(|I_{rs}^\alpha|^2\Big(\frac{1}{6}+\frac{1}{6}\frac{M_F^2}{(m_r+m_s)^2}\Big)+|J_{rs}^\alpha|^2\Big(\frac{1}{6}+\frac{11}{6}\frac{M_F^2}{(m_r+m_s)^2}\Big)\Big)\right]. \quad (5.106)$$

Here, $M_F$ is the mass of the meson, $f_F$ is its decay constant and $B_F$ are recalibration constants of order 1, related to vacuum insertion formalism. Lastly, $m_r$ and $m_s$ are the masses of the quarks of which the meson is build, i.e. $rs = bd, bs, ds$ stands for $B_d$, $B_s$ and $K^0$ respectively. Recent experimental values for the meson parameters, including $\Delta M_F$ that should be reproduced by the model, are given in table 5.11.3

| Meson | $M_F$ (GeV) | $f_F$ (GeV) | $B_F$ | $\Delta M_F$ (GeV) |
|---|---|---|---|---|
| $B_d$ ($\bar{b}d$) | 5.2795 | $0.1928 \pm 0.0099$ | $1.26 \pm 0.11$ | $(3.337 \pm 0.006) \times 10^{-13}$ |
| $B_s$ ($\bar{b}s$) | 5.3664 | $0.2388 \pm 0.0095$ | $1.33 \pm 0.06$ | $(1.170 \pm 0.008) \times 10^{-11}$ |
| $K$ ($\bar{s}d$) | 0.497614 | $0.1558 \pm 0.0017$ | $0.725 \pm 0.026$ | $(3.500 \pm 0.006) \times 10^{-15}$ |
| $D$ ($\bar{u}c$) | 1.8648 | 0.165 | 0.82 | $(0.95 \pm 0.37) \times 10^{-14}$ |

Table 5.5: *Properties of neutral mesons (from [158] for $B_d$, $B_s$ and $K$ and from [157] for $D$).*

We stress that the tests developed in this section do not constitute a complete list. Many other other processes can be thought of. The ones considered in this section already prove to be very constraining as shown in the next section when we apply them to the models described in the previous section.

## 5.12 Results of the model dependent tests

The tests developed in the previous section can be applied to the four models described in section 5.10. Of course we apply the lepton tests to models 1 and 2 and the meson oscillation tests to model 3. For model 4 we focus on the addition of quarks to the model and we apply the meson oscillation tests also here. Furthermore we study the effect of the new dimension-6 operators on the relic density of the dark matter candidate.

### 5.12.1 Model 1

Discussion of the flavour violating processes in model 1 is best done in terms of the fields $\varphi$, $\varphi'$ and $\varphi''$ in the $Z_3$ eigenstate basis of section 5.6.2. In the context of lepton triality, this was discussed before in [159]. Furthermore, the transformation properties of the additional scalar $\eta$ allow a mixing between $\varphi^0$ ($\varphi^1$) and $\eta^0$ ($\eta^1$), both behaving as the SM-Higgs. However, this mixing interaction, $iZ\eta^0\varphi^0 + h.c.$, that was not present in section 5.6.2, is irrelevant for the scalar spectrum discussion, because the coupling, being suppressed by $v_\eta$, is extremely small .

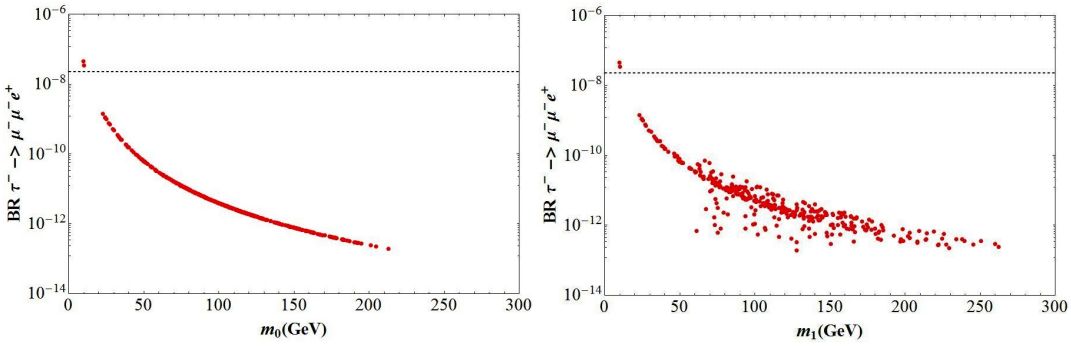


Figure 5.12: *The branching ratio for the decay $\tau^- \to \mu^-\mu^-e^+$ in model 1 as a function of the effective mass $m_0$ (left) and the smallest mass $m_1$ (right) in the situation where the parameter $\epsilon$ is zero. The horizontal line corresponds to the experimental upper bound.*

The coupling of the Higgses $\varphi'^0$, $\varphi''^0$ to fermions is purely flavour violating. This setup has striking effects on the lepton processes. In fact it was shown in [160] that, when the $A_4$ symmetry is unbroken, only a limited number of processes is allowed and these either conserve flavour or satisfy the

constraint $\Delta L_e \times \Delta L_\mu \times \Delta L_\tau = \pm 2$. The only source of symmetry breaking is the vev of the SM-like Higgs $\varphi^0$, which is flavour-conserving and thus not involved in the processes we are looking at. We conclude that all flavour violating processes should satisfy the selection rule. In particular this implies that the decays $\mu^- \to e^- e^- e^+$ and $\mu \to e\gamma$ are not allowed, in the latter case in contrast with what was reported in [97], but in agreement with the more recent [161].

Of the allowed processes, $\tau^- \to \mu^- \mu^- e^+$ is least suppressed, since its branching ratio is proportional to $m_\tau^2 m_\mu^2$. However, even this decay is very rare and below the experimental limit for most values of the Higgs masses. In the upper part of figure 5.12, we plot the branching ratio for the decay against an effective mass defined as $m_0^{-2} = m_{h_A}^{-2} + m_{h_B}^{-2}$, where $A$ and $B$ are the two pairs of degenerate bosons. In the lower part, the same branching ratio against the mass of the lightest state, $m_1$. In both the plots, the parameter $\epsilon$ is set to zero, corresponding to the real Higgs potential discussed in [97]. For the first picture, we reproduce the result of [97] that the branching ratio is proportional to $m_0^{-4}$. In the second one, this dependence is lost, even if we can see a similar behaviour. Once we take $\epsilon$ over the full range $[0, 2\pi]$, we verified that the points cover a larger parameter space, but still concentrating around the previous points with $\epsilon = 0$.

In figure 5.13, we show the masses of the SM-Higgs $\varphi^0$, $m_{h_1}$, against the mass of the lightest state $m_1$. A plot with the mass of the SM-Higgs $\eta^0$ against $m_1$ looks very similar to figure 5.13. All the points are above the diagonal and this corresponds to the fact that the SM-Higgses are always heavier than the lightest state. As already mentioned in section 5.9.1, there is no upper bound on the mass of the SM-like Higgs mass. In particular the standard upper bound of $194$ GeV at $99\%$ CL [6] does not apply, due to the combined effect of the CP and $Z_3$ symmetries and the smallness of the $iZ\eta^0\varphi^0 + h.c.$ coupling.

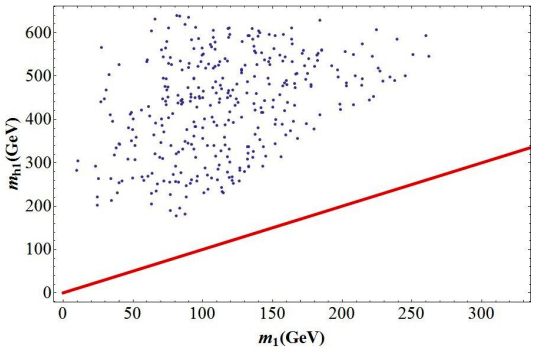


Figure 5.13: *The mass of the SM-like Higgs $m_{h_1}$ against the smallest Higgs mass $m_1$ in model 1.*

### 5.12.2 Model 2

In contrast with the Model 1, $A_4$ is completely broken by the vev of the Higgs triplet. As there is no residual symmetry, there are no special selection rules that forbid flavour changing interactions. In particular the processes $\mu^- \to e^- e^- e^+$ and $\mu^- \to e^- \gamma$ are allowed. The first process, figure 5.14 occurs at tree level and produces a strong bounds on the Higgs sector, where the lightest Higgs mass is expected to be above about 300 GeV. On the other hand, the radiative muon decay to an electron, figure 5.14, is loop suppressed and the new physics leads to a branching ratio below the observed experimental bound.

### 5.12.3 Model 3

Experimentally, in the quark sector two features have been explored: flavour changing interactions and CP violation. Remarkably, the CKM matrix obtained in the model under inspection is completely

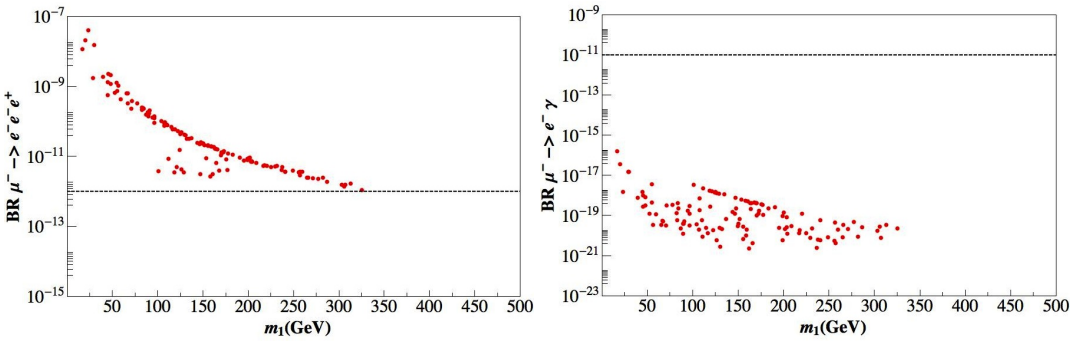


Figure 5.14: *The branching ratio of the decay of $\mu^- \to e^- e^- e^+$ (left) and $\mu^- \to e^- \gamma$ (right) in model 2 versus the lightest Higgs mass. The horizontal band is the experimental limit [6].*

real. It seems then of scarce value to explore CP violating effects coming from the complex vevs of the Higgs triplet, not having the dominant contribution from the Standard Model CKM matrix to compare them with. Consequently we only focus on flavour changing processes. As discussed in section 5.11.3 meson oscillations are in these models mediated by tree level diagrams instead of box diagrams. We therefore expect strong bounds from the mass splittings in the neutral B-meson and Kaon systems. In figure 5.15, we plot $\Delta M_F$ versus the lightest Higgs mass for these systems. Indeed $\Delta M_F$ is large, up to several orders of magnitude above the experimental value for the $B_d$ meson and the Kaon.

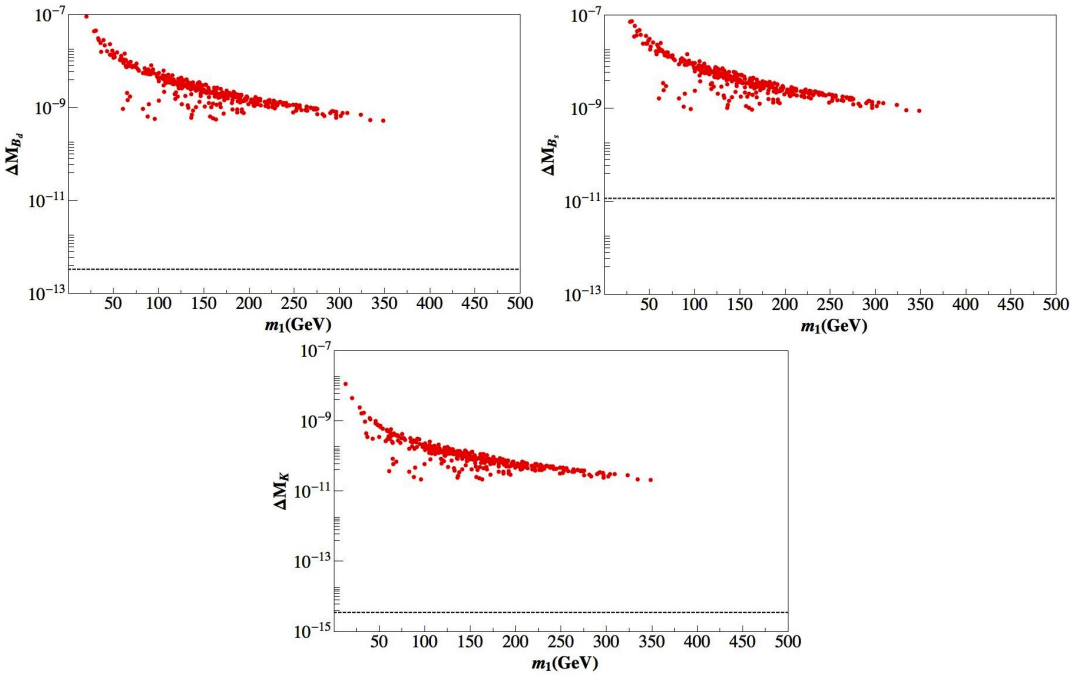


Figure 5.15: *$\Delta M_F$ for $B_d$, $B_s$ and $K$ mass splittings versus the lightest Higgs mass in model 3. The horizontal lines correspond to the experimental values as reported in [158].*

### 5.12.4 Model 4 - Quark mixing in the discrete dark matter model

In section 5.10.4 we discussed how adding effective dimension-6 operators to the original discrete dark matter model allowed the quarks to mix according to the CKM matrix. These operators also

allow flavour changing neutral currents and in particular meson-antimeson oscillations, that occur through diagrams given in figure 5.16, challenge the validity of our extension of the model.

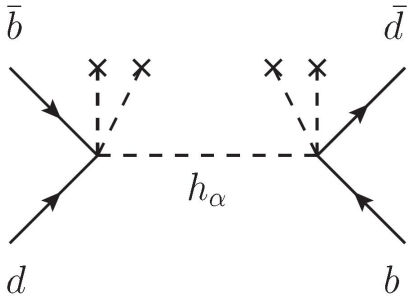


Figure 5.16: *In model 4, $B_d$ and other meson oscillations can occur through a special version of the diagram on the right of figure 5.11.*

As mentioned in the section 5.10.4, the CKM matrix can dominantly originate from corrections to the up-type quark mass matrices or the down-type quark mass matrices and we mentioned that dominance of the latter is more natural. Indeed we find that if corrections of the former type dominate or even if there is no dominance of one of the two, the contribution to $\Delta M_D$ of $D$ meson oscillations given only by the new diagrams is much larger than the experimental value [157] and this scenario should be excluded as shown in figure 5.17.

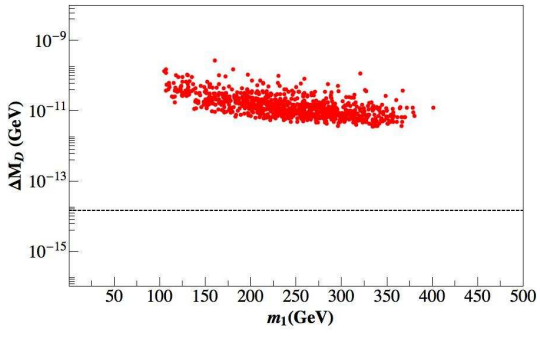


Figure 5.17: *$D$ meson oscillations in model 4 in a scenario where the CKM matrix is generated dominantly by corrections to the up-type quark mass matrix.*

In case the CKM matrix mostly originates from corrections to the down-type quark mass matrix, we find that the bounds from meson mixing are rather strong. In figure 5.18, we show the contribution of the new diagrams to $\Delta M_{B_d}$, $\Delta M_{B_s}$ and $\Delta M_K$ as function of the lightest Higgs mass. We see that in almost all of parameter space the points are near or even above the short-dashed line, which indicates the current experimental value [158] that is rather well described by the Standard Model box diagrams [6, 162]. Naively, this is interpreted as an exclusion of the model, which is true in most of parameter space, but not in points where the Standard Model and new physics contributions partially cancel. To see this, we write the mixing amplitude for $B_d$ mixing as [163]

$$\left[M_{12}^d\right]_{\rm NP} = (1 - \frac{1}{1 + h_d^2 e^{2i\sigma_d}})\left[M_{12}^d\right]_{\rm full} \tag{5.107}$$

and analogously for $B_s$. We have verified that our expression for the NP contribution carries enough phases to generate a flat distribution for $\sigma_d$ and $\sigma_s$. We check that the points in $(h_d^2 = 0.41, \sigma_d = 100^\circ)$ and $(h_s^2 = 1.6, \sigma_s = 90^\circ)$ are allowed by the data [163, 164] and give a nett contribution of NP with respect to the full result of respectively 0.65 and 2.67 times the observed value. For $B_d$ mesons, NP effects are thus forced to be less than the observed value, while for $B_s$ mesons, it can even be slightly more. These values (and a corresponding estimate in case of the kaons) correspond to the dot-dashed

lines in 5.18. We see that a small, but significant number of points is allowed by the data under the assumption of partial cancellation.

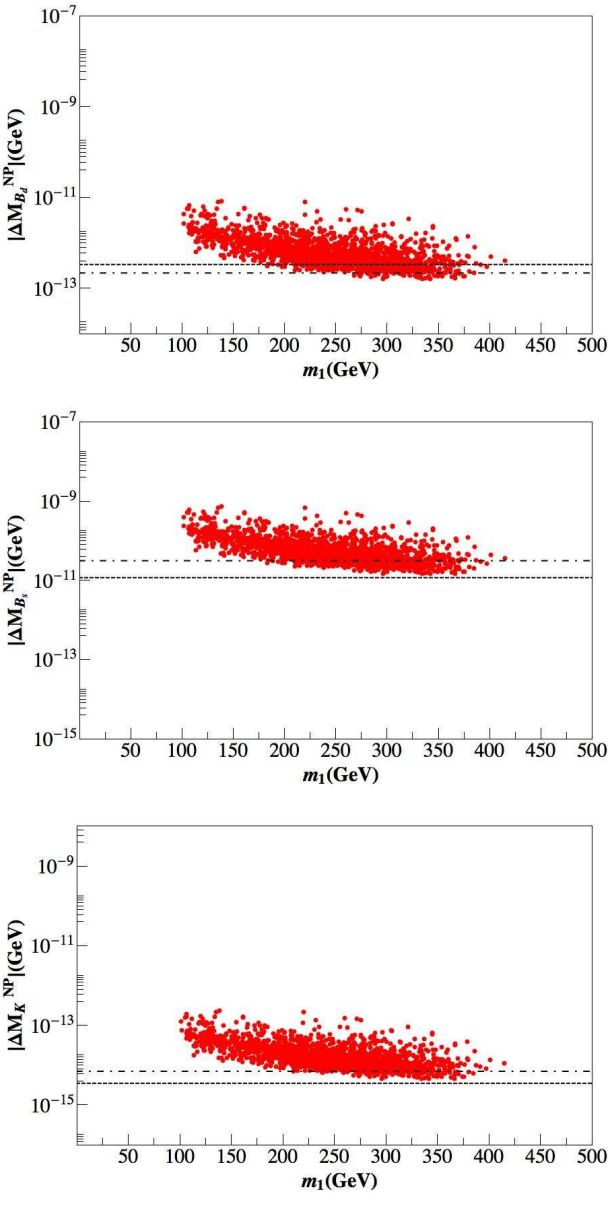


Figure 5.18: *B and K mesons oscillations. The horizontal lines are as explained in the text.*

The naturalness of this cancellation, that requires finetuning between the phase and amplitude of the new and the Standard Model contribution, can be a matter of debate. The need for cancellation diminishes for larger Higgs masses, although there are still no points below the lower line for $B_s$ and $K$. Indeed, requiring that the new diagrams contribute less than the experimental bound, as is customarily done, the model would be excluded. On the other hand allowing a strong negative interference between the SM and the DDM contributions does not further constrain the scalar spectrum with respect to the analysis done in [152]. Indeed figure 5.19 shows that there is no correlation between the bound imposed and the mass of the lightest $Z_2$-even scalar state, even if the number of points allowed is significantly reduced with respect to the earlier analysis.

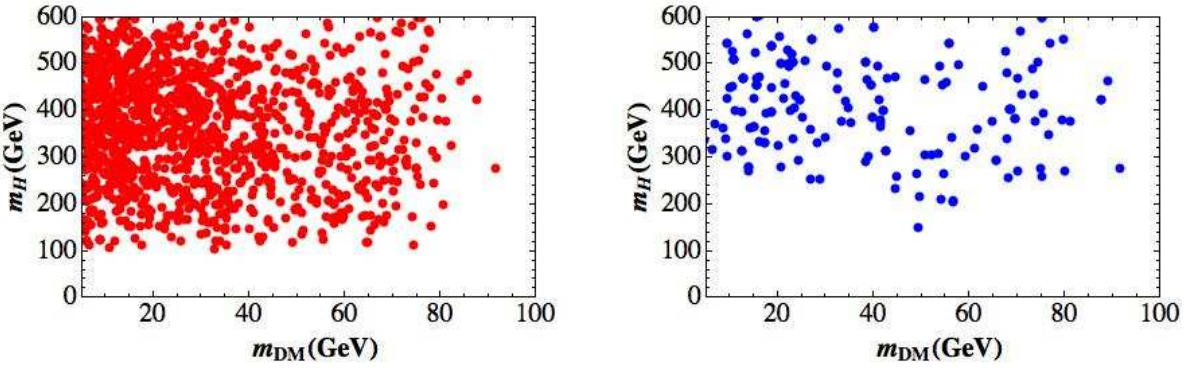


Figure 5.19: *The mass of the lightest $Z_2$-even state of model 4 versus the mass of the DM candidate without (red) and with (blue) meson oscillation constraints.*

**Dark matter relic density and direct detection**

Here we consider the effect of the inclusion of the dimension-six terms of equation (5.94) to the relic density. The operators (5.94) give an effective quartic coupling of the dark matter with quarks. This enhances the annihilation of the dark matter candidate into quark pairs that in the original model is only possible via SM Higgs exchange in the s-channel. We only study the decay into down quarks; decay to up quarks is barely affected as we have seen that $D$-meson constraints force the off-diagonal elements in the up-type quark mass matrix to be very small.

We define the $\lambda^q_{eff}$ as the parameter of the four points interaction $\chi\chi d_i\bar{d}_j$ - i.e. the result of the three couplings in (5.94) when $H$ but not the two $\eta$s obtain their vevs. We can use equation (5.96) to estimate its size. The assumption is that all $h$s are of the same natural order of magnitude as the $h_{ds}$ of equation (5.96). An important exception may be $h_{dd}$ that needs to be small in order not to inflate the down mass. For all other couplings, we find

$$\lambda^d_{eff} \sim h^d_{ij}\frac{v_H}{\Lambda^2} \sim \frac{m_s\lambda_C}{v_\eta^2}\,. \tag{5.108}$$

We compare the effect of this operator on the $\sigma v_{rel}$ of the process $\chi\chi \to d_i\bar{d}_i$ to the effect of $s$-channel exchange of the SM-like lightest CP-even scalar. The SM-like Higgs couples to fermions proportionally to $y_q \sim m_q/v_H$. The new contribution is negligible if

$$\frac{m_s\lambda_C}{v_\eta^2} < \frac{m_q A_H}{v_H m_h^2}\,. \tag{5.109}$$

In this equation $m_h$ is the mass of the lightest CP-even neutral scalar and $A_H \sim v_{\rm ew}$ is the dimensional coupling that controls the interaction of the dark matter with the Higgs doublet $H\chi\chi$. Since

$v_\eta \sim v_H \sim m_h \sim A_H \sim v_{\rm ew}$ the new contribution is naturally subleading for the second and third generation. For the first generation, on the contrary the new contribution to $\chi\chi \to d\bar{d}$ is of the same order as the old one. We can (conservatively) estimate that this channel is negligible only for values $M_{DM} \geq 1\,\text{GeV}$. This is basically satisfied for all values of the dark matter mass, that we reported to be in the range 1 - 100 GeV in section 5.10.4.

Direct detection is not affected at all by the NLO terms: the quark flavour diagonal scattering contribution are subdominant with respect to those mediated by the scalar $H$ while the off-diagonal one could only give rise to processes that are not kinematically allowed such as $\chi + \mathcal{N} \to \chi + \mathcal{N} + \pi^+ + e^- + \bar{\nu}$, with $\mathcal{N}$ a nucleus in the detector bulk.

This concludes the discussion of the quark extension of the discrete dark matter model. Relic density and direct detection calculations do not constrain its viability. Meson oscillations do. $D$ meson oscillations exclude any significant off-diagonal elements in the up-quark mass matrix. Kaon and $B_s$ meson oscillations also produce very tight constraints. These do not immediately rule out the set up, but the model can only be in accordance with the experimental data if there is significant finetuning between Standard Model and new physics contributions. All together, honesty forces us to say that this 'natural extension' is less natural then we hoped.

## 5.13 Conclusions of the chapter

Flavour models based on non-Abelian discrete symmetries under which the SM scalar doublet (and its replicates) transforms non trivially are quite appealing for many reasons. First of all there are no new physics scales, since the flavour and the EW symmetries are simultaneously broken. Furthermore this kind of models are typically more minimal with respect to the ones in which the flavour scale is higher than the EW one: in particular the vacuum configuration is simpler and the number of parameters is lower. We then expect a high predictive power and clear phenomenological signatures in processes involving both fermions and scalars.

In this chapter we focussed on the $A_4$ discrete group, but this analysis can be safely generalized for any non-Abelian discrete symmetry. We consider three copies of the SM Higgs fields, that transform as a triplet of $A_4$. This setting has already been chosen in several papers [97, 127, 128, 150–152, 159] due to the simple vacuum alignment mechanism. In each of these works, a certain configuration has been assumed for the vacuum expectation values of the three Higgs bosons.

In this chapter we have considered all the possible vacuum configurations allowed by the $A_4 \times SM$ scalar potential. These obviously contain the vacua studied in earlier models. We showed furthermore that the total list is rather small. The potential allows only the five minima mentioned in section 5.6.9 and permutations of their components.

The fact that a certain vev combination is a true minimum of the Higgs potential does not automatically imply that a model that uses three Higgs fields with these vacuum expectation values is physically viable. In this chapter we described two groups of tests to check if a model is in accordance with the current (pre-LHC) data. The first group of tests only considers the Higgs sector. It is not influenced by the choice of $A_4$ representations for the fermions, only by the representation choice for the Higgs fields, that are fixed to be in the triplet representation of $A_4$. We considered constraints by unitarity, by $W$ and $Z$ decays, and by the oblique parameters $S$, $T$ and $U$. For all but one vacua considered, a significant number of points passed all three tests. The exception is one of the complex vacua. This can only be realistic if the $A_4$-invariant Higgs potential is extended with some terms that break the family symmetry softly. This makes models that use this vacuum significantly less attractive.

The second group of tests consists of processes in which the fermions participate and for which it is thus needed to know the $A_4$ representations of these fields. We developed a very general formalism to describe the interaction of charged and neutral Higgs and of fermions. In the mass basis of both Higgs bosons and fermions the interaction depends on the Yukawa matrices that appear in the

Lagrangian and the unitary matrices that rotate the flavour basis into the mass basis. When these matrices are given, a number of flavour violating processes can be calculated and these calculations can be used to test the viability of models in the literature.

We showed that for three of the four models considered in detail in this chapter, flavour violating processes significantly reduce the viability of the set up. It is not a coincidence that he only model for which the flavour changing neutral currents do not pose a large problem, assumes the Higgs fields to be in the configuration with the maximal residual symmetry.

In conclusion, we showed that for flavour models with the family symmetry implemented at the electroweak scale, it is possible to test their phenomenology beyond the prediction of the mixing patterns. This is a powerful tool to discriminate among them. Indeed, many Higgs vacuum configurations and concrete models considered in this chapter can be strongly constrained or almost ruled out. The fact that this falsification is possible is most important advantage of the set up of flavour symmetries at the electroweak scale.

# Appendix to chapter 5

## 5.A Analytical formulæ for the oblique parameters

In this appendix we provide a dictionary from the notation in the original papers introducing the oblique parameters [141, 144] to ours.

In the notation of Peskin and Takeuchi, we are in the case in which $n_d = 3$ and $n_n, n_c = 0$; this implies that the matrices $\mathcal{T}$ and $\mathcal{R}$ are vanishing. The quantities that need to be translated are

$$\begin{aligned} \mathcal{U} &\rightarrow S \\ \mathrm{Re}\mathcal{V}_{ki} &\rightarrow U_{ki}\,, \\ \mathrm{Im}\mathcal{V}_{ki} &\rightarrow U_{k+3i}\,, \\ \omega_k &\rightarrow f_k e^{i\omega_k}\,. \end{aligned} \tag{5.A.1}$$

Moreover they put the GBs as first mass eigenstates while we put them as the last ones and contrary to them we use the standard definition for the photon.

We have rewritten the expression for

$$\frac{A(I,J,Q)-A(I,J,0)}{Q} = \begin{cases} dA(I,J) & \text{for } I \neq 0 \text{ and/or } J \neq 0\,, \\ \dfrac{QF(Q)}{Q} \sim \dfrac{1}{48\pi^2}\log Q & \text{for } I = J = 0 \text{ since } A(0,0,0) = 0\,. \end{cases} \tag{5.A.2}$$

In the first row of equation(5.A.2) we used

$$A(I,J,Q) \simeq A(I,J,0) + Q\frac{\partial A(I,J,Q)}{\partial Q}\bigg|_{Q=0} = A(I,J,0) + Q\,dA(I,J)\,. \tag{5.A.3}$$

In this expression $dA(I,J)$ is given by

$$dA(I,J) = \begin{cases} \dfrac{1}{288(I-J)^3\pi^2}\left[I^3 + 9JI^2 + 6(I-3J)\log(I)I^2 - 9J^2I - J^3 + 6(3I-J)J^2\log(J)\right] \\ \qquad\qquad \text{for } I, J \neq 0, I \neq J\,, \\ \dfrac{1}{288\pi^2}(1 + 6Log[I]) \qquad \text{for } J = 0\,, \\ \dfrac{1}{48\pi^2}(1 + \log[I]) \qquad \text{for } I = J\,. \end{cases} \tag{5.A.4}$$

The function $\bar{A}(I,J,Q)$ enters only in the loops in which a gauge boson and a scalar run, so we have always $J = Q$ when computing the quantity

$$\frac{\bar{A}(I,J,Q)-\bar{A}(I,J,0)}{Q} = \bar{dA}(I,J)\,. \tag{5.A.5}$$

As a result, for this function, it does not make sense to consider the case $I = J = 0$ where $J = Q = m_V^2$ the gauge boson mass. Eventually we find

$$d\bar{A}(I,Q) = \begin{cases} \frac{1}{8(I-Q)^3\pi^2}\left[Q\left(-I^2 + 2Q\log(I)I - 2Q\log(Q)I + Q^2\right)\right] & \text{for } I \neq Q, I \neq 0\,, \\ \sim 0 \qquad\qquad\qquad\quad \text{for } I = 0\,, \\ \sim 0 \qquad\qquad\qquad\quad \text{for } I = Q\,. \end{cases} \tag{5.A.6}$$